Quaternary Geochronology 43 (2018) 50–71

Contents lists available at ScienceDirect

Quaternary Geochronology

journal homepage: www.elsevier.com/locate/quageo

Untangling geochronological complexity in organic spring deposits using multiple dating methods

Emily Field[a,*], Sam Marx[b], Jordahna Haig[c,d], Jan-Hendrik May[e,f], Geraldine Jacobsen[g], Atun Zawadzki[g], David Child[g], Henk Heijnis[g], Michael Hotchkis[g], Hamish McGowan[a], Patrick Moss[a]

[a] School of Earth and Environmental Sciences, University of Queensland, Australia
[b] GeoQuEST Research Centre, School of Earth and Environmental Sciences, University of Wollongong, Australia
[c] College of Science, Technology & Engineering, James Cook University, Australia
[d] ARC Centre of Excellence for Australian Biodiversity and Heritage, Australia
[e] School of Geography, University of Melbourne, Australia
[f] Department of Earth Sciences, University of Freiburg, Germany
[g] Australian Nuclear Science and Technology Organisation, Lucas Heights, Australia

ARTICLE INFO

Keywords:
Organic spring
Carbon-14
Hydrogen pyrolysis
Lead-210
Plutonium-239 + 240
L_n/T_n

ABSTRACT

Organic spring deposits have the potential to provide to outstanding records of palaeoenvironmental and climatic change, particularly in arid and semi-arid environments where establishing robust records of environmental change is challenging due to a lack of classic sedimentary records, e.g. perennial lakes and extensive wetlands. However, despite the potential of organic spring deposits a number of studies demonstrate complications in the application of standard ^{14}C techniques which has, in several cases, led to confusing chronologies. This implies that dynamic carbon pathways commonly occur within spring systems. Because of the importance of springs as critical palaeoenvironmental archives, this study sought to better understand the behaviour of ^{14}C and other radionuclides used in geochronology within organic springs, and ultimately, establish a protocol for building reliable chronologies in these environments. To do this, we utilised multiple geochronological methodologies to investigate cores collected from three springs in the Kimberley region of northwest Australia. This included ^{14}C dating of different carbon fractions, ^{210}Pb dating, the application of $^{239+240}Pu$, and novel, high spatial resolution, luminescence techniques as indicators of geochronological structure. The natural sensitivity-corrected luminescence (L_n/T_n) signal indicated the studied springs contained a relatively complete stratigraphic record, however ^{14}C results were found to be convoluted by contamination attributed to a combination of roots, groundwater fluctuations and allochthonous input of "old" carbon affecting ages. Whilst it was found that no single carbon fraction is universally reliable in dynamic spring environments, dating the stable polycyclic aromatic carbon (SPAC), isolated by hydrogen pyrolysis (HyPy) pre-treatment, appeared to remove the effects of post-depositional modification which otherwise perturbed the age of carbon fractions with respect to sedimentary development of the spring. By contrast, the ability of ^{210}Pb and $^{239+240}Pu$ to provide detailed chronologies for recent spring sediments (i.e. the past 100 years) was found to be complicated due to the behaviour of springs as an open system with regards to uranium. Therefore, it may not be possible to construct ^{210}Pb chronologies in many spring environments. Overall, the results of this study indicate that it is possible to construct ^{14}C based chronologies in spring systems, however it is necessary to understand the effects of physical and biological processes within springs on ^{14}C pathways. In particular, the application of HyPy pre-treatment of SPAC appears to offer a viable approach to constructing chronologies in these environments. Furthermore, although this study pertains to springs, the sources of geochronological complexity described here are not exclusive to these systems and our results are therefore more widely applicable.

* Corresponding author.
E-mail address: e.field@uq.edu.au (E. Field).

http://dx.doi.org/10.1016/j.quageo.2017.10.002
Received 8 April 2017; Received in revised form 19 September 2017; Accepted 9 October 2017
Available online 13 October 2017

1. Introduction

Perennial or ephemeral springs are important palaeoenvironmental archives, particularly in otherwise arid or semi-arid environments (Boyd and Luly, 2005). The use of springs for palaeoenvironmental research requires the preservation of a record within the sediments or organic deposits that accumulate around the spring vent. Organic deposits are particularly valuable in this context as they preserve a range of palaeoecological proxies, including palynomorphs (pollen and non-pollen), diatoms, molluscs, charcoal, plant macrofossils and humic acids (e.g. Scott, 1982a; Van de Geer et al., 1986; Dodson and Wright, 1989; Boyd, 1990b; Macphail et al., 1999; Owen et al., 2004; Dobrowolski et al., 2005; Dobrowolski et al., 2012; McGowan et al., 2012; Fluin et al., 2013; Backwell et al., 2014; Dobrowolski et al., 2016; Field et al., 2017). Typically, organic sediments such as peat are formed in saturated and low oxygen conditions since this minimises the rate of decomposition. However, in many springs artesian pressure sustains a water-table "dome" higher than the surrounding terrain, allowing organic material to accumulate above ground at spring vents when evaporation rates are lower than spring discharge (Ponder, 1986; Boyd, 1990a; McCarthy et al., 2010). Whilst under artesian pressure, capillary creep and slow outward diffusion of groundwater throughout these deposits is sufficient to maintain moisture levels minimising oxidation and desiccation (McCarthy et al., 2010). In addition to palaeoecological indicators organic spring deposits can preserve a range of other palaeoenvironmental information such as stable isotope ratios, geochemical tracers and rates of dust deposition through time (e.g. Dobrowolski et al., 2005; Dobrowolski et al., 2012, 2016; McGowan et al., 2012; Mazurek et al., 2014).

In arid and semi-arid environments establishing continuous records of Quaternary environmental change is challenging due to the lack of perennial water sources (e.g. lakes) that preserve robust sedimentary records. Records from those water bodies that do exist, such as ephemeral lakes, commonly contain chronological hiatuses, for example during dry periods when deposition may cease, or unconformities due to aeolian deflation and scouring during heavy rainfall and floods (Head and Fullager, 1992; Magee et al.,2004). In addition, these environments have limited fossil preservation due to oxidation during dry periods. As such, important palaeoenvironmental and climatic information has been derived from organic springs in the arid and semi-arid environments of Australia (e.g. Dodson and Wright, 1989; Boyd, 1990b; McGowan et al., 2012; Fluin et al., 2013; Field et al., 2017), Kenya (e.g. Owen et al., 2004), Jordan (Rambeau, 2010) and South Africa (e.g. Scott, 1982a, 1988,b; Scott and Vogel, 1983; Van Zinderen Bakker, 1989; Scott and Cooremans, 1990; Scott and Nyakale, 2002; Truc et al., 2013), with some records spanning up to ~37,000 years (e.g. Fluin et al., 2013). For instance, pollen analysis at Wonderkrater spring mound has yielded a ~35,000 year record of climatic evolution (Scott, 1982b), and more recently quantitative climatic estimates from pollen-transfer functions (Truc et al., 2013), whilst diatom-transfer functions from a spring at the Campground Wetlands in Kenya have been used to provide pH, conductivity and temperature estimates for part of the late Holocene (Owen et al., 2004). Spring deposits have also been shown to be viable traps for aeolian dust. For example, a ~6500 year record of dust accumulation was constructed for Black Springs, one of the study sites investigated in this paper (McGowan et al., 2012). In that study, patterns in dust flux through time were used to investigate changing moisture regimes which were linked to changing patterns in the Australian monsoon. Outside of arid and semi-arid regions, springs within larger mire complexes have also been used to reconstruct valuable palaeoenvironmental records, for example in Poland (e.g. Dobrowolski et al., 2005; Dobrowolski et al., 2012, 2016; Mazurek et al., 2014) and Australia (e.g. Van de Geer et al., 1986; Macphail et al., 1999), with some records encompassing at least ~52,000 years (e.g. Van de Geer et al., 1986). Since springs are a focus of human and faunal activity in water scarce regions they are also an important source of palaeontological and archaeological information. Consequently, occupational and faunal remains have been found surrounding springs (e.g. Hughes and Lambert, 1985; Veth, 1989) and within their sediments (e.g. Potezny, 1978; Kuman and Clarke, 1986; Backwell et al., 2014) up to ~138,000 years before present (BP) (e.g. Backwell et al., 2014). Springs have particular importance in arid Australia and feature prominently in the songlines and myths of Indigenous Australians (Harris, 2002). They were also of strategic importance to early European explorers in Australia, acting as vital "stepping stones" across the arid interior of the continent (Harris, 1981).

Despite the potential of organic spring deposits as excellent archives of palaeoenvironmental and climatic information, there are a number of complications in the application of standard radiocarbon (^{14}C) techniques. This, in many cases, has led to confusing chronologies in springs (e.g. Scott and Vogel, 1983; Kuman and Clarke, 1986; Scott, 1987; Boyd, 1990a; Macphail et al., 1999; Scott et al., 2003; Dobrowolski et al., 2012; Mazurek et al., 2014; Field et al., 2017) (see Section 1.2; Figs. 2 and 3) which may compromise the integrity of environmental, climatic, palaeontological and archaeological reconstructions.

The aim of this study was to establish a protocol for building reliable chronologies for organic spring deposits through the analysis of dates generated using multiple methodologies, utilising springs from the Kimberley region of northwestern Australia as an example. The Kimberley is also of importance as there remains a limited understanding of palaeoenvironmental and climatic change in Australia's tropical savannah (Reeves et al., 2013). It is also an area within which multiple organic springs have been identified (e.g. Department of Environment and Conservation, 2012; Field et al., 2017) and is an environment where there are few other opportunities to construct detailed chronological records of the recent past. Ages from three springs in the Kimberley are obtained via accelerator mass spectrometry (AMS) and standard radiometric ^{14}C dating with acid-alkali-acid (AAA) and hydrogen pyrolysis (HyPy) pre-treatments on a number of carbon fractions (pollen concentrate, macro-charcoal, bulk organics, stable polycyclic aromatic carbon (SPAC) and roots). For the uppermost sediments, chronological control is attempted using lead-210 (^{210}Pb) and plutonium-239 + 240 ($^{239+240}$Pu) analysis. Supporting chronological information is provided by analysis of the polonium-210 (^{210}Po) and radium-226 (^{226}Ra) activities of groundwater, macro-charcoal investigation, and the application of luminescence techniques at high spatial resolution (natural sensitivity-corrected luminescence (L_n/T_n)). The ability to build reliable chronologies for organic spring sediments is important to enable researchers to obtain accurate, high resolution palaeoclimate and environmental records. This is of particular concern in arid and semi-arid regions which are typically challenging for Quaternary research. Additionally, reliable chronologies from organic spring deposits will facilitate improved interpretation of the age of cultural and faunal artefacts found in their sediments.

1.1. Conceptual sources of geochronological complexity in organic spring deposits

Within organic springs there are a number of processes that have the potential to complicate the geochronological integrity of sedimentary deposits (Fig. 1). These processes include aeolian and alluvial input, root growth, upwelling groundwater, weathering, bioturbation, and mass movement within the spring.

Allochthonous transport of biological material to the spring by aeolian or alluvial processes has the potential to introduce "old" carbon, affecting ^{14}C ages. This can include "old" charcoal which may remain in the surrounding landscape due to its presumed long-term environmental persistence, despite some evidence suggesting that it may not be as stable as originally thought (see Bird, 2007 and references within). The protuberant morphology of the spring mound above the surrounding landscape reduces the likelihood of "old" carbon

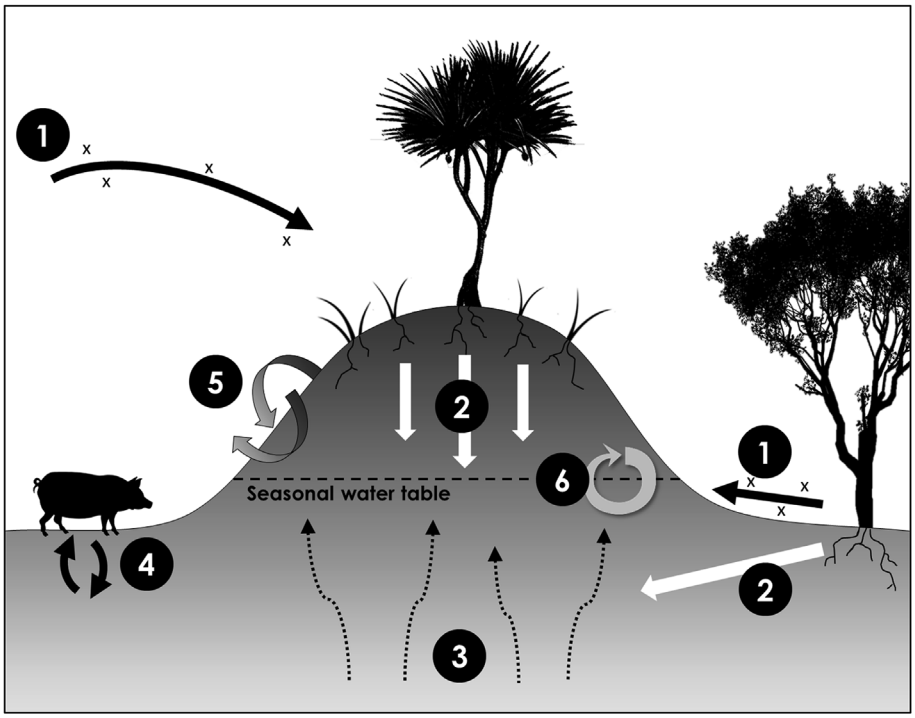

Fig. 1. Potential sources of geochronological complexity in organic springs via (1) aeolian and alluvial input, (2) root growth and washdown of organic substances and sediment, (3) upwelling groundwater, (4) bioturbation, (5) self-mulching, slumping, and (6) weathering.

washing into the spring sediments. However, alluvial input may occur during the spring's early stages before development of a mound (Ponder, 1986; Field et al., 2017), or during large floods when the mound is small but prone to inundation. Over time charcoal in the landscape may be broken down into finer fractions (Walker, 2005; Bird, 2007) which can then be blown into the spring during any stage of its development. Transport of “old” carbon into springs by these mechanisms may compromise their age structure.

Perennial springs, or those where oxygenated ground water supports enhanced plant growth, can contain deep rooted vegetation (Scott and Vogel, 1983) introducing young carbon into the spring deposits (Boyd, 1990b). Depending on the fraction dated, this young carbon cannot easily be removed from other biological fractions since separation methods (e.g. density separation or acid digestion) will also affect the organics targeted for ^{14}C dating. Removing rootlets by hand is extremely time consuming and not possible in all cases. Rootlets can also penetrate large charcoal fragments selected for dating by growing along the original wood fibres (Harkness et al., 1994), thereby compromising the age of the charcoal fragment. In addition, the decay of roots can facilitate transport of young biological material or sediment via root channels affecting geochronology. These root channels may also allow the movement of other radiological sediment markers such as ^{210}Pb and $^{239+240}$Pu to shift downwards in the profile.

In springs upwelling groundwater is related to meteoric recharge (McCarthy et al., 2010). During periods of decreased rainfall a lower water table can facilitate desiccation of the organic sediments (Scott, 2016). If springs then become dry, aeolian deflation may remove part of the deposit, while onset of rainfall could result in downward transport of sediment and biological substances through the peat matrix. In addition, springs may also experience cracking and self-mulching leading to mixing and overturning of mound stratigraphy. Alternatively, during periods of high spring discharge there is potential for upward movement of sediment and biological material, whilst sediments may also be removed via scouring during the spring's early stages before a mound develops. These processes may cause ^{14}C, ^{210}Pb, fallout radionuclide and luminescence results to be unreliable.

Water table fluctuations can cause *in-situ* alterations to charcoal preserved in the sediments (e.g. Bird et al., 2002) affecting returned ^{14}C ages. Because of the large surface area and porous nature of charcoal it lends itself to adsorption of various organic and inorganic compounds (Bird, 2007). This makes it an ideal substrate for microbial colonisation which allows continued carbon cycling between fossilised charcoal and the modern environment (Zackrisson et al., 1996), and facilitates replacement of the original carbon by various oxides and oxihydroxides (Bird et al., 2002). Charcoal may also undergo oxidative degradation (Cohen-Ofri et al., 2006), particularly in coarser matrixes, as a result of bacterial activity and weathering, which may occur during periods when the water table is lower. It has been demonstrated that removal of charcoal contamination with ^{14}C pre-treatments such as AAA or even the more rigorous acid-base-oxidation with stepped combustion (ABOX-SC) methodology is not always effective (e.g. Gillespie et al., 1992; Harkness et al., 1994; Bird et al., 2002; Higham et al., 2009a,b), particularly in high weathering environments, where contaminants can irreversibly react with, and alter, the charcoal surface (Bird, 2007). Charcoal in organic spring deposits may therefore be contaminated with young carbon, particularly in cases where there have been large water table fluctuations.

Upwelling groundwater through organic spring deposits can also render them open systems in regards to uranium, which may be leached from host rocks/sediments and transported in solution within groundwater (Sirocko et al., 2007). This can affect U-series dating, including ^{210}Pb. Organic decomposition products such as fulvic and humic acids are capable of adsorbing large quantities of uranium, which bind strongly to clay minerals in organic sediments (Szalay, 1969; Van der Wijk et al., 1986). Therefore the decomposition of organic matter and low redox potential of peat deposits make them ideal environments for the geochemical trapping of uranium (Shotyk, 1988). This can result in uranium-enriched organic deposits (e.g. Heijnis, 1992; Heijnis and van der Plicht, 1992; Zayre et al., 2006) even where relatively low concentrations of uranium are observed in the groundwater (e.g. Armands, 1967). Uranium and associated daughter products such as ^{210}Po and ^{226}Ra can therefore be high in organic spring sediments which may complicate the use of ^{210}Pb as a geochronological tool by masking unsupported ^{210}Pb activities.

Internal physical processes within springs can also influence their age stratigraphy. This includes slumping of the spring mound, if they

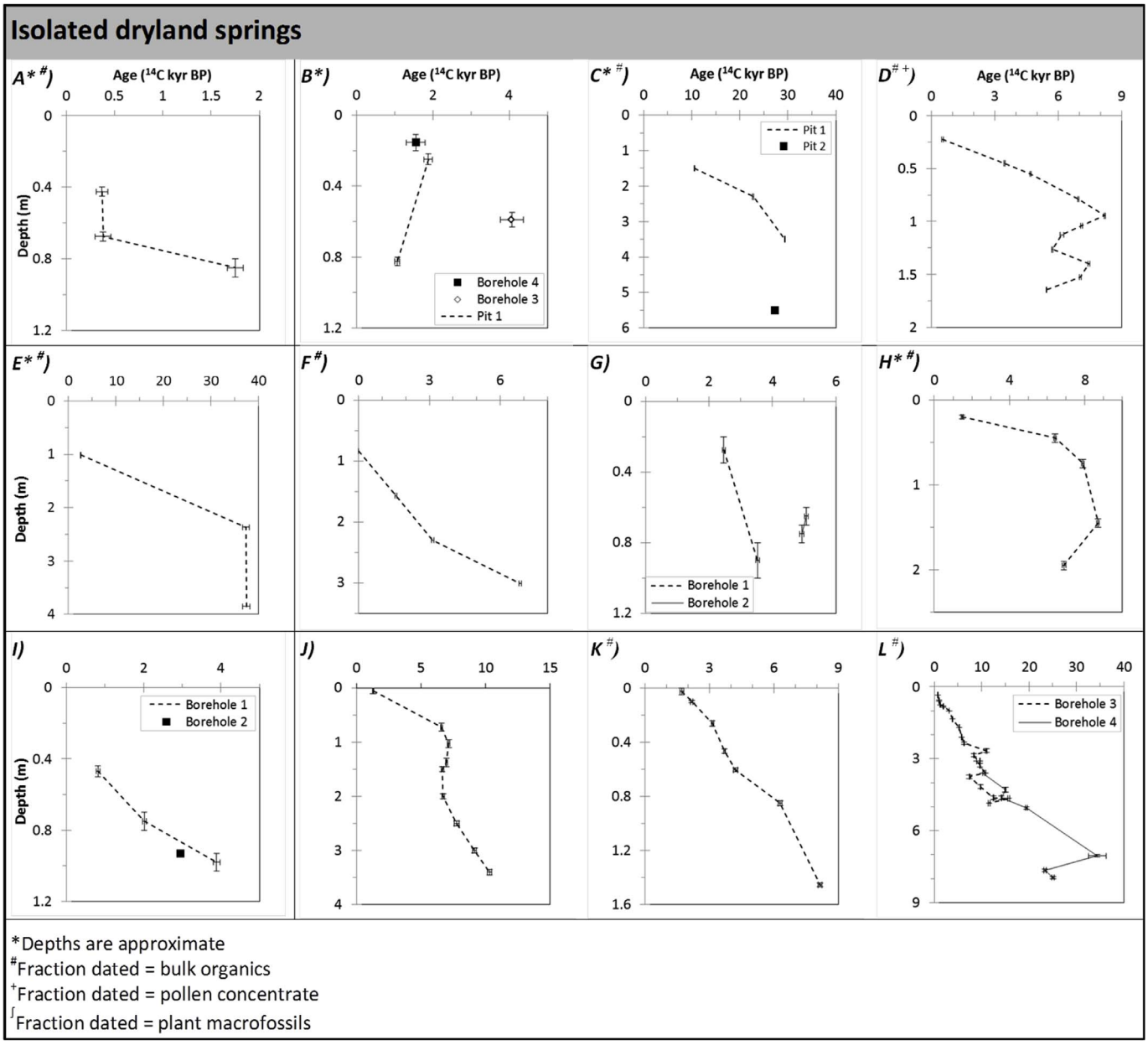

Fig. 2. Carbon-14 chronologies from (A) Dalhousie Springs, Australia (Boyd, 1990b), (B) Uitzigt, South Africa (Butzer, 1984a,b), (C) Ulungra Springs, Australia (Dodson and Wright, 1989), (D) Black Springs, Australia (Field et al., 2017), (E) Warburton Spring, Australia (Fluin et al., 2013), (F) EDSA, Jordan (Rambeau, 2010), (G) Scot, South Africa (Scott, 1982b), (H) Tate Vondo, South Africa (Scott, 1987), (I) Meriba Spring, South Africa (Scott, 1988), (J) Rietvlei, South Africa (Scott and Vogel, 1983), (K) Florisbad Spring, South Africa (Scott and Nyakale, 2002) and (L) Wonderkrater, South Africa (Scott et al., 2003).

develop too steeply, or if the vent position changes. As a focal point for animals, springs can also be affected by bioturbation (Scott, 2016). In Australia, this may be more pronounced after the arrival of Europeans and the introduction of domestic livestock, which occurred from the 1800s in the Kimberley.

1.2. Common chronological issues in organic spring deposits

Existing palaeoenvironmental records from organic springs overwhelmingly rely on ^{14}C dating, however the majority of published ^{14}C chronologies are complicated by age-depth reversals and/or erroneously young dates. This is demonstrated in Figs. 2 and 3, which depict age-depth profiles characteristic of organic springs presented in earlier published works, both from isolated dryland springs (Fig. 2) and from springs within larger mire complexes (Fig. 3) (see figure captions for publication details). The plotted profiles come from a variety of global locations (Fig. 4), in which the carbon fraction dated consists predominantly of either bulk organics or pollen concentrate, with the exception of Dalhousie Springs, Scot, Meriba Springs and Rietvlei (Fig. 2A, G, 2I and 2J) where the carbon fraction dated is unknown, and Zawadówka, Mowbray Swamp and Pulbeena Swamp (Fig. 3M, T and 3U) where a number of other fractions were analysed including macrofossils, root stumps and humic extracts.

The chronologies of the plotted records are predominantly characterised by either sudden increases in age over narrow depth intervals (Figs. 2A and 3N), unreasonably high sedimentation rates (Fig. 2A, E and 3O), or more commonly age reversals (Fig. 2B, D, 2G, 2H, 2J, 2L, 3M, 3N, 3P - R). The latter implies complexity of carbon sources within the springs, while the former could represent contamination of the preceding layer with younger carbon, or perhaps indicate unconformities or growth hiatuses in the springs as a result of aeolian deflation or scouring. Age reversals are also seen in the Mowbray

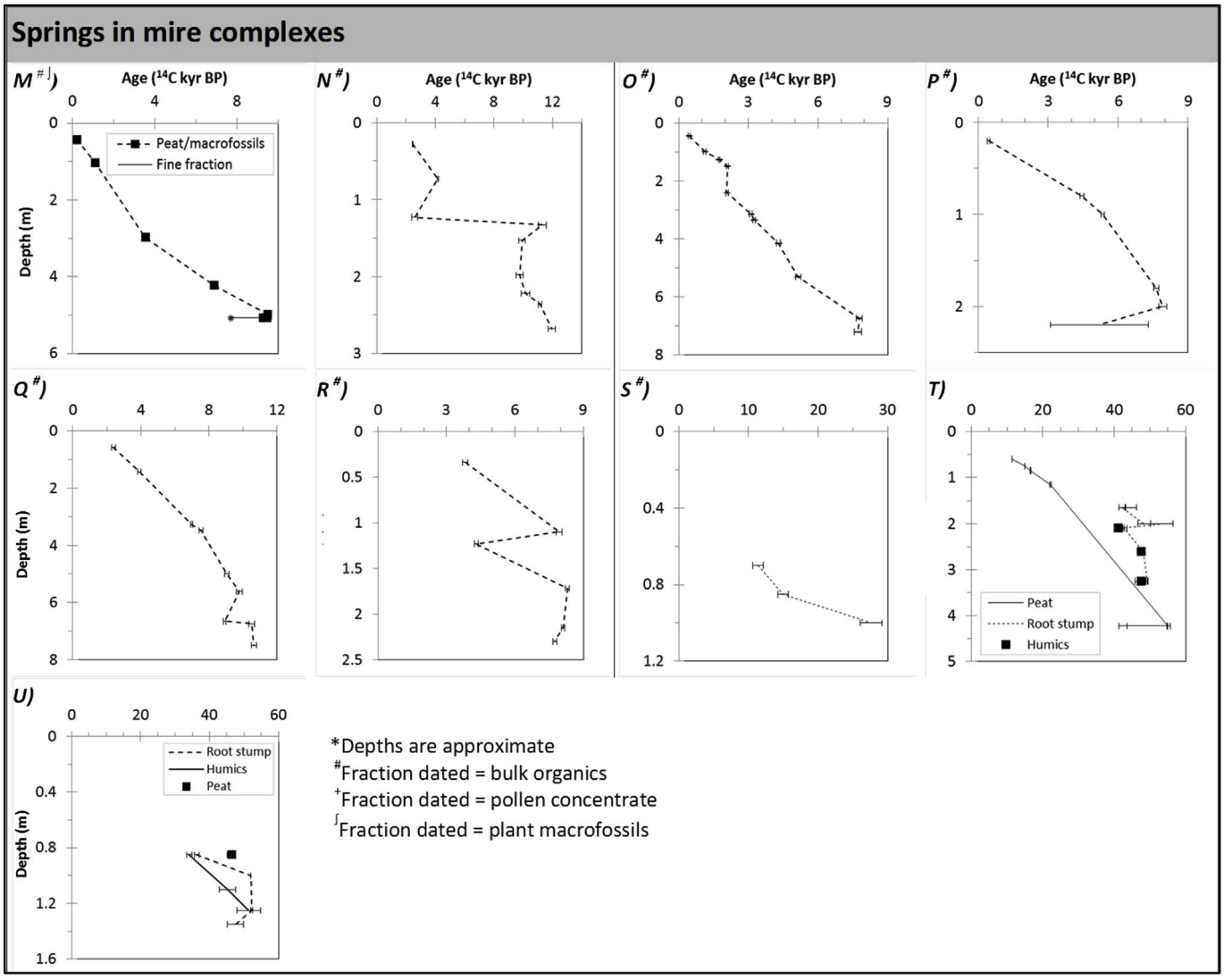

Fig. 3. Carbon-14 chronologies from (M) Zawadówka, Poland (Dobrowolski et al., 2005), (N) Radzików, Poland (Dobrowolski et al., 2012), (O) Komarów, Poland (Dobrowolski et al., 2016), (P) Melaleuca Tin Mine, Australia (Macphail et al., 1999), (Q) Bobolice, Poland (Mazurek et al., 2014), (R) Orgartowo, Poland (Mazurek et al., 2014), (S) Broadmeadow Swamp, Australia (Van de Geer et al., 1986), (T) Mowbray Swamp, Australia (Van de Geer et al., 1986) and (U) Pulbeena Swamp, Australia (Van de Geer et al., 1986).

Swamp and Pulbeena Swamp chronologies (Fig. 3T and U) and whilst the authors note the presence of trace contamination at these sites, these reversals may be due in part to dates being near the ^{14}C barrier (Van de Geer et al., 1986). There are also a number of examples where ages are contradictory between corresponding cores or pits surveyed at the same site and similar depth (Fig. 2B, C, 2G and 2L).

The extent of complications in ^{14}C chronologies within organic springs is further illustrated by the fact that, to the best of our knowledge, there are just four published studies where the spring chronology is free from complications (Fig. 2F, I, 2K and 3S). In one of these studies at Florisbad Spring, South Africa, an earlier study had previously found erratic ^{14}C ages which were attributed to contamination of ^{14}C by roots (Kuman and Clarke, 1986). In the later study of Scott and Nyakale (2002), a concerted effort to remove root fragments from bulk organic ^{14}C was undertaken, resulting in a coherent age-depth profile for the site, i.e. ages increased with depth (Fig. 2K). Therefore, although existing studies have highlighted the value of organic spring deposits as palaeoenvironmental archives, to the best of our knowledge, in most cases the information contained is convoluted by the problematic geochronology.

2. Physical setting

Sediment cores from three springs in the northwest Kimberley are analysed in this study; Black Springs, Fern Pool and Gap Springs. The springs are located along a broadly north-south transect approximately 100 km in length (Fig. 5), with Black Springs furthest north at 15.633°S, 126.389°E, Fern Pool at 15.937°S, 126.284°E, and Gap Springs furthest south at 16.404°S, 126.134°E. The climate is monsoonal with a mean annual rainfall of ~1000 mm/yr. When combined with a mean annual potential evapotranspiration of ~1900 mm/yr and high seasonality (> 70% of precipitation falling between January and March) (Bureau of Meteorology, 2016) this creates a water-limited environment within which these springs occur.

Of the studied springs, Black Springs has the most prominent mound (approximately 2 m in height above the surrounding landscape), while Fern Pool is less elevated above the landscape and Gap Springs has no topographic protuberance. These differences in mound morphology are likely attributable to discharge, with Black Springs having more vigorous groundwater discharge by comparison to Fern Pool and Gap Springs. The springs are heavily vegetated in contrast to the surrounding tropical savanna, with taxa growing across them including *Phragmites* (a perennial aquatic grass), sedges (Cypereaceae), *Melaleuca*

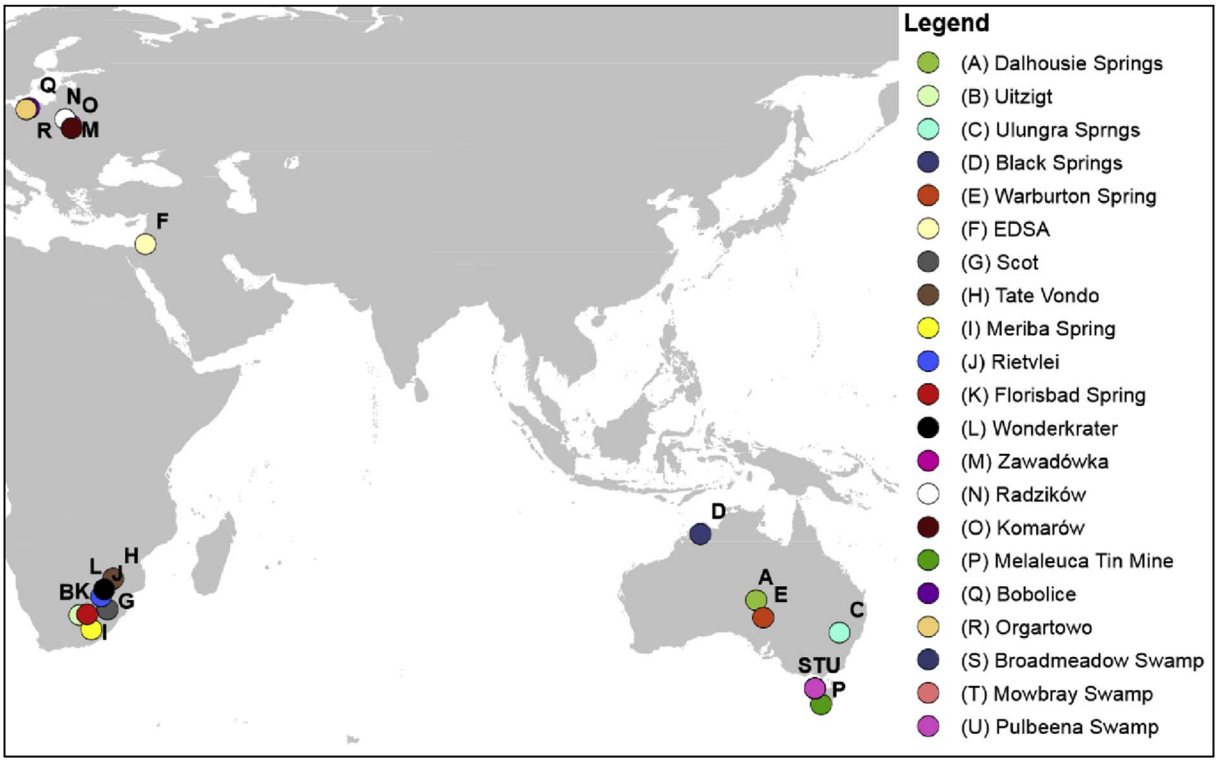

Fig. 4. The location of springs plotted in Fig. 2 and 3.

and *Pandanus spiralis*. At Black Springs the vegetation is particularly dense with the mound also covered by monsoon vine thicket including *Ficus* and *Timonius timon* (Department of Environment and Conservation, 2012 and field observation), whilst *Banksia dentata* is prevalent at Gap Springs.

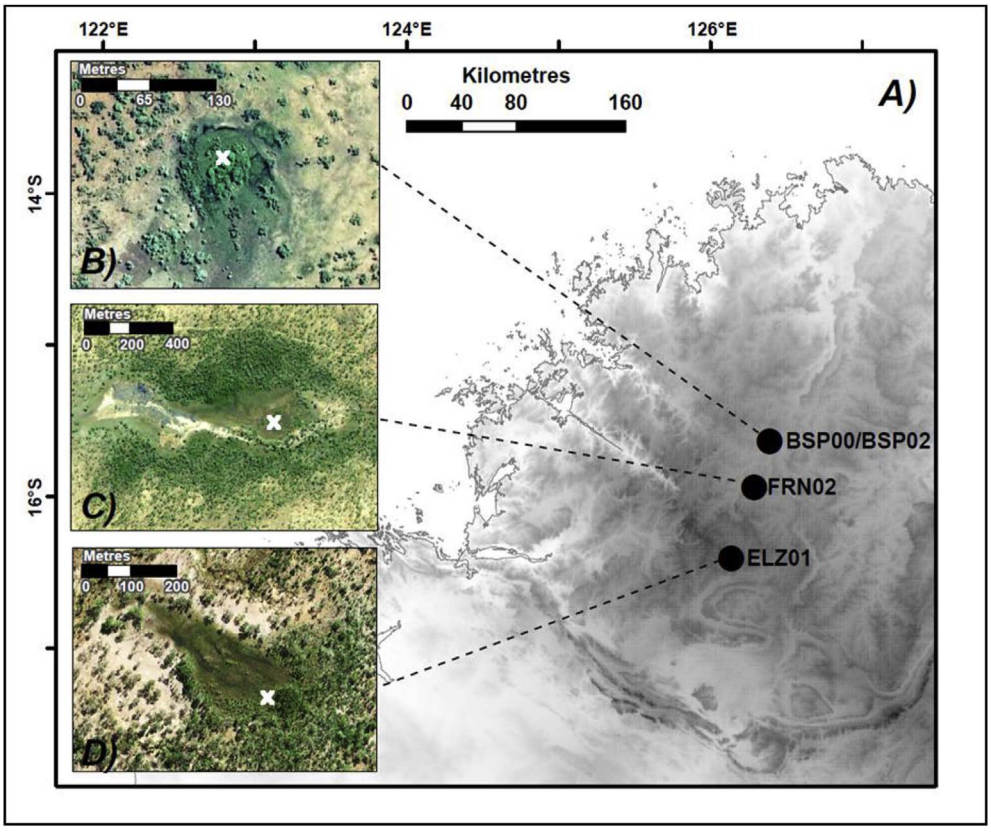

Fig. 5. Location of the three springs investigated in this study. An overview map is shown in panel (A), whilst satellite imagery of the three sites are shown for Black Springs (BSP02/BSP00) in panel (B), Fern Pool (FRN02) in panel (C), and Gap Springs (ELZ01) in panel (D). Coring locations are indicated by a white cross.

3. Materials and methods

3.1. Core collection and description

The three springs examined in this study (Black Springs, Fern Pool and Gap Springs) were cored during the Kimberley's dry season in June, 2015 using a 50 cm long Russian D-section corer. A core was also collected from Black Springs in 2005 (BSP00) and was previously described in McGowan et al. (2012) and Field et al. (2017). Ages from that core are presented here for comparison. Cores BSP02, FRN02 and ELZ01 were photographed on the ITRAX micro X-ray Fluorescence (μXRF) core scanner at the Australian Nuclear Science and Technology Organisation (ANSTO) before being described using standard stratigraphic techniques including Munsell colour and field-texture analysis. Organic content of the cores were determined by Loss-on-Ignition (LOI) following Heiri et al. (2001).

3.2. Carbon-14 dating

In this study, four carbon fractions; pollen concentrate, macro-charcoal, stable polycyclic aromatic carbon (SPAC) and roots were dated by ^{14}C. Carbon stable isotope ratios were determined using an Isotope Ratio Mass Spectrometer (IRMS $\delta^{13}C$) for ^{14}C measurement correction. No macrofossils suitable for ^{14}C dating were found.

In BSP02, FRN02 and ELZ02 initial samples of pollen concentrate and macro-charcoal were extracted at the same, or similar, depths wherever possible to facilitate comparisons between results. Sample locations were selected where radiograph imagery indicated minimal root disturbance. Some initial macro-charcoal and pollen concentrate dates contained inconsistencies and age reversals (see Fig. 7), so to help clarify core geochronology and better understand the source of ^{14}C inconsistencies in the springs SPAC was also extracted from selected depths throughout BSP02, FRN02 and ELZ01. During density separation of pollen concentrate, we noted that small root fragments floated off along with the pollen. It was considered that these roots may have introduced younger ^{14}C, increasing the ^{14}C:^{12}C ratio and decreasing pollen concentrate ages. For this reason, roots from the basal pollen samples of BSP02 and FRN02 were extracted for dating for comparison with the ages returned on SPAC and charcoal fractions.

For core BSP00, dates were obtained on pollen concentrate and bulk organic fractions. To better understand ^{14}C sources in this core, two bulk organic samples (humins) were also dated, one by standard ^{14}C radiometric techniques (Wk-41825) and one by AMS due to its small sample volume (Wk-41826).

All samples were calibrated using the OxCal program (V4.2.4.) (Bronk Ramsey, 2013) and the Southern Hemisphere calibration curve (SHCal13) (Hogg et al., 2013), with 0 cal yr BP representing 1950 AD.

3.2.1. Pollen concentrate

Extraction of pollen for dating was adapted from the method outlined in Moss (2013). Seventeen sediment samples (three from both BSP02 and FRN02, two in ELZ01, and nine in BSP00) were disaggregated with 10% sodium pyrophosphate ($Na_4P_2O_7$) for 1 h then passed through a series of sieves (2 mm, 500 μm, 150 μm and 8 μm diameter mesh) to collect roots (> 2 mm and 500 μm fractions) and pollen (< 150 μm and > 8 μm fraction). Unwanted inorganic material was removed from the pollen via density separation with sodium polytungstate ($Na_6H_2O_{40}W_{12}$) at specific gravity 1.9. In addition the 2015 core samples were cleaned with 40% hydrofluoric acid (HF) to remove residual silicates. Remaining organics were washed in Milli-Q water and retained for ^{14}C analysis.

Pollen concentrate samples were pre-treated using the AAA technique following Hatté et al. (2001). Sequential washings of hydrochloric acid (HCl) to remove carbonates, repeated sodium hydroxide (NaOH) washes to remove fulvic and humic acids, and HCl to remove any atmospheric carbon dioxide (CO_2) absorbed during alkali treatment, were performed. Samples were combusted at 900 °C to convert them to CO_2, followed by graphitisation using the H_2/Fe method (Hua et al., 2001). Carbon-14 measurement of pollen concentrate from BSP02, FRN02 and ELZ01 was undertaken by AMS on the ANTARES and STAR accelerators at ANSTO (Fink et al., 2004), whilst pollen concentrate from BSP00 was submitted to Waikato Radiocarbon Dating Laboratory for processing with AMS measurement undertaken at the W.M Keck Carbon Cycle Accelerator Mass Spectrometry Laboratory, University of California.

3.2.2. Macro-charcoal

Extraction of macro-charcoal followed the method outlined in Stevenson and Haberle (2005). Ten samples (four from both BSP02 and FRN02, two from ELZ01) were disaggregated with 10% $Na_4P_2O_7$ heated to 100 °C, then passed through a 125 μm sieve with the > 125 μm fraction retained. The retained samples were treated with 6% hydrogen peroxide (H_2O_2) to bleach organic material and facilitate identification of charcoal. Charcoal was identified under a binocular microscope and hand-picked into Milli-Q water using titanium high precision tweezers. The picked charcoal was dried at 60 °C with a target dry weight of > 2 mg assuming some material would be lost during AAA pre-treatment. Samples were pre-treated using AAA, combusted and graphitised as described in Section 3.2.1 and were measured by AMS at ANSTO.

3.2.3. Bulk organics

Two bulk organic samples from BSP00 were submitted to Waikato Radiocarbon Dating Laboratory. Visible contaminants were removed before samples were pre-treated using AAA, combusted and graphitised as described in Section 3.2.1. Sample Wk-41826 was measured for ^{14}C by AMS (as previously described) whilst the larger mass of sample Wk-41825 enabled it to be measured by Liquid Scintillation Spectrometry on a Perkin Elmer 1220 “Quantulus” Liquid Scintillation (LS) spectrometer.

3.2.4. Stable polycyclic aromatic carbon (SPAC)

HyPy is a relatively new ^{14}C pre-treatment methodology, where samples undergo pyrolysis aided by high hydrogen pressures in the presence of a dispersed sulphided molybdenum catalyst (Ascough et al., 2009). This method isolates the SPAC component of a sample by removing > 92% of the labile organic material including contaminants (Ascough et al., 2009; Bird et al., 2014). Twelve samples (three from FRN02, four from BSP02 and five from ELZ01) were treated by HyPy at James Cook University following the approach of Ascough et al. (2009) and Meredith et al. (2012). Aliquots of each sample (~1 g) were loaded with a dispersed sulphided molybdenum catalyst (~10% by weight) using an aqueous MeOH solution of ammonium dioxydithiomolybdate ($\{NH_4\}_2MoO_2S_2$), sonicated for 15 min, then dried overnight at 70 °C in a vacuum oven. These samples were placed in the HyPy reactor, pressurized with hydrogen (H_2) to 150 bar with a gas flow of 4 L/minute. The HyPy residues were combusted and graphitised as described in Section 3.2.1 and measured by AMS at ANSTO.

3.2.5. Roots

Roots > 2 mm retained during sieving for the pollen fraction were collected from the basal sample of both BSP02 and FRN02. Samples were submitted to Beta Analytic where they were pre-treated using AAA, combusted and graphitised as described in Section 3.2.1 and measured by AMS.

3.3. Lead-210 dating

Eight samples through the top 70 mm in BSP02 and FRN02 and 18 samples through the top 310 mm in ELZ01 were dated using ^{210} Pb at ANSTO. Sediment ages were determined from unsupported ^{210}Pb activity using the constant initial concentration (CIC) (Robbins and Edgington, 1975) and constant rate of supply (CRS) (Appleby and

Oldfield, 1978) models. Supported ^{210}Pb was determined by measuring ^{226}Ra, while total ^{210}Pb was determined by measuring ^{210}Po, both of which are assumed to be in secular equilibrium with ^{210}Pb. Unsupported ^{210}Pb activity was calculated as the difference between supported ^{210}Pb and total ^{210}Pb activity. Samples were dried at 60 °C for 48 h in order to calculate moisture content, with dry bulk density calculated using Equation (1). Separation and analysis of ^{226}Ra and ^{210}Po began by adding isotopic tracers of barium-133 (^{133}Ba) and polonium-209 (^{209}Po) to 0.2 g dried sediment. Samples were digested in a combination of nitric acid (HNO_3), H_2O_2 and HCl to extract ^{226}Ra and ^{210}Po from the sample matrix. Polonium-209 + 210 were auto-deposited onto silver disks and counted by high resolution alpha spectrometry, whilst ^{226}Ra and ^{133}Ba were co-precipitated with barium sulfate ($BaSO_4$) and collected on membrane filters. Barium-133 was counted on a high purity germanium (HPGe) gamma detector to determine its recovery which is used to estimate the recovery of ^{226}Ra. The activity of ^{226}Ra was determined by high resolution alpha spectrometry. Sample ages were corrected for moisture content and dry bulk density.

$$\rho = \frac{S_{wm}}{S_{wv}}\left(1 - \frac{\theta_s}{100}\right) \quad (1)$$

ρ = Dry bulk density (g/mL); S_{wm} = Sample wet mass (g); S_{wv} = Sample wet volume (m^3); θ_s = Sample moisture content (%)

3.4. Plutonium-239 + 240 chronostratigraphic markers

Plutonium-239 + 240 activities in ELZ01 and BSP02 were analysed as an additional chronostratigraphic marker. These isotopes have the same anthropogenic source as caesium-137 (^{137}Cs), i.e. derived from nuclear weapon test fallout, however they have a longer half-life (24,110 years for ^{239}Pu) and 6561 years for ^{240}Pu compared to 30 years for ^{137}Cs (Browne and Tuli, 2006, 2007, 2014) enabling detection in far smaller sediment masses. In addition, $^{239+240}$Pu analysis by AMS has a better sensitivity than ^{137}Cs measured by gamma spectrometry. Plutonium-239 + 240 activities are therefore ideal as chronological markers for identifying the period between the early 1950s and 1964, i.e. the beginning and peak of nuclear weapons testing fallout. Plutonium-239 + 240 activities were measured in nine samples in the top 130 mm in ELZ01 and six samples in the top 90 mm in BSP02. Samples were prepared following Child et al. (2008) whereby they were ashed at 800 °C to remove organic soil components, plutonium-242 (^{242}Pu) and uranium-233 (^{233}U) were added as isotope dilution tracers, leached with 10 mL aqua regia (3:1 HCl:HNO_3) to solubilize stratospheric fallout Pu, then purified by ion extraction chromatography (Eichrom TEVA® resin). The separated Pu was co-precipitated with iron (III) oxide-hydroxide ($Fe\{OH\}_3$), then dried and calcined to form an iron oxide matrix for AMS analysis. Measurement was undertaken by AMS on the VEGA accelerator at ANSTO (Wilcken et al., 2015). PuO^- ions were injected into the accelerator which was operated at 0.6 MV. Using helium gas stripping Pu^{3+} ions were selected for analysis after acceleration, yielding greater than 30% particle transmission efficiency. Plutonium-230 + 240 are quantified relative to the known amounts of ^{242}Pu added to each sample by measurement of the 239/242 and 240/242 isotope ratios.

3.5. Supporting chronological information

3.5.1. Luminescence analysis

Twenty five samples from BSP02 were analysed with a modified luminescence screening approach (e.g. Sanderson and Murphy, 2010; Munyikwa and Brown, 2014) to determine whether mixing of the sediment profile or subtle stratigraphic breaks could be responsible for the erratic age-depth relationships frequently observed in organic spring ^{14}C chronologies. Sediment samples were extracted in a dark room under red light at 5–10 cm intervals from the central portion of the core to reduce the risk of light exposure. These samples were then digested in a dark-room in 6% H_2O_2. Three 6 mm aliquots from each sample were prepared on steel discs from the remaining detrital material.

To enable direct comparability between aliquots while allowing time effective measurement as necessary for achieving high spatial resolution through the core, the first cycle of standard post-IR OSL SAR protocols (e.g. Murray and Wintle, 2000; Wintle and Murray, 2006) were measured on a Lexsyg smart device (Richter et al., 2013) at the University of Freiburg, Germany. The natural luminescence signal (L_n) was measured by preheating the aliquots to 210 °C for 10 s prior to all measurements, followed by 100 s of infra-red stimulation (IRSL, 850 nm peak emission, 130 mW cm-2), and 40 s of blue light stimulation (BSL, 458 nm peak emission, 50 mW cm-2). The IRSL signal was recorded for 85 s while the BSL signal was recorded for 40 s with a Hoya-U340 filter in combination with a Delta-BP 365/50 Interference Filter. Additionally, a Schott NG-4 AHF Brightline HC414/46 Interference filter and a Schott NG-11 filter were used to avoid overexposure for particularly bright aliquots. A test signal (T_n) was subsequently determined by repeating the measurement after an application of a beta test dose of 99 Bs. The first 8 and 0.6 s of the recorded IRSL and BSL signals, respectively, were used for integration by subtracting the signal between and 75–85 s (IRSL) and 25–30 s (BSL) as background. The down-core variation of the resulting normalized luminescence signal (L_n/T_n ratio) was then interpreted.

3.5.2. Examination of macro-charcoal

Due to inconsistencies in the macro-charcoal ^{14}C dates (as presented in Section 4.2), charcoal sub-samples from the ^{14}C samples were examined for charcoal alteration. Fragments were examined by scanning electron microscopy (SEM) with element distributions obtained via SEM energy dispersive X-ray analysis (EDXA) on a Hitachi TM3030 desktop SEM with Bruker EDS at the University of Queensland.

3.5.3. Polonium-210 and radium-226 activities of groundwater

The activities of ^{210}Po and ^{226}Ra were measured in the groundwater at each of the three springs to assess if U-series isotopes in groundwater could be affecting sediment ^{210}Pb activities. Samples of spring water were collected from each site during the 2015 field campaign, with 50 mL of each sample passed through a 0.45 μm filter. Both the filtrate (groundwater) and residue (organic material) from each sample were analysed by alpha spectrometry for ^{210}Po and ^{226}Ra activities using the method described in Section 3.3 at ANSTO.

4. Results

4.1. Core lithology

Sedimentary sequences for BSP02, FRN02 and ELZ01 are shown in Fig. 6. The BSP02 core (242 cm) collected from Black Springs consists of approximately 80 cm of black, well decomposed peat (70% organic content by weight). Between 80 and 175 cm the organic content decreases down-core whilst the clay content increases. A marked change to organic silty clay occurs at 175 cm (organic content < 20%), with the silty clay content increasing below 200 cm (organic content < 10%).

The FRN02 core (204 cm) collected from Fern Pool consists of a 10 cm root mat, underlain by brown, poorly decomposed peat. At 55 cm the degree of peat decomposition increases and the peat becomes darker. At 125 cm there is a change to organic silty clay, the colour of which becomes lighter grey with depth. The lower portion of the core contains TiO/Al_2O_3 concretions (below 124 cm).

The ELZ01 core (140 cm) collected from Gap Springs consists of a short organic layer (up to 50% organic content) at the top of core (0–25 cm). Below this the core consists of grey organic silty clay

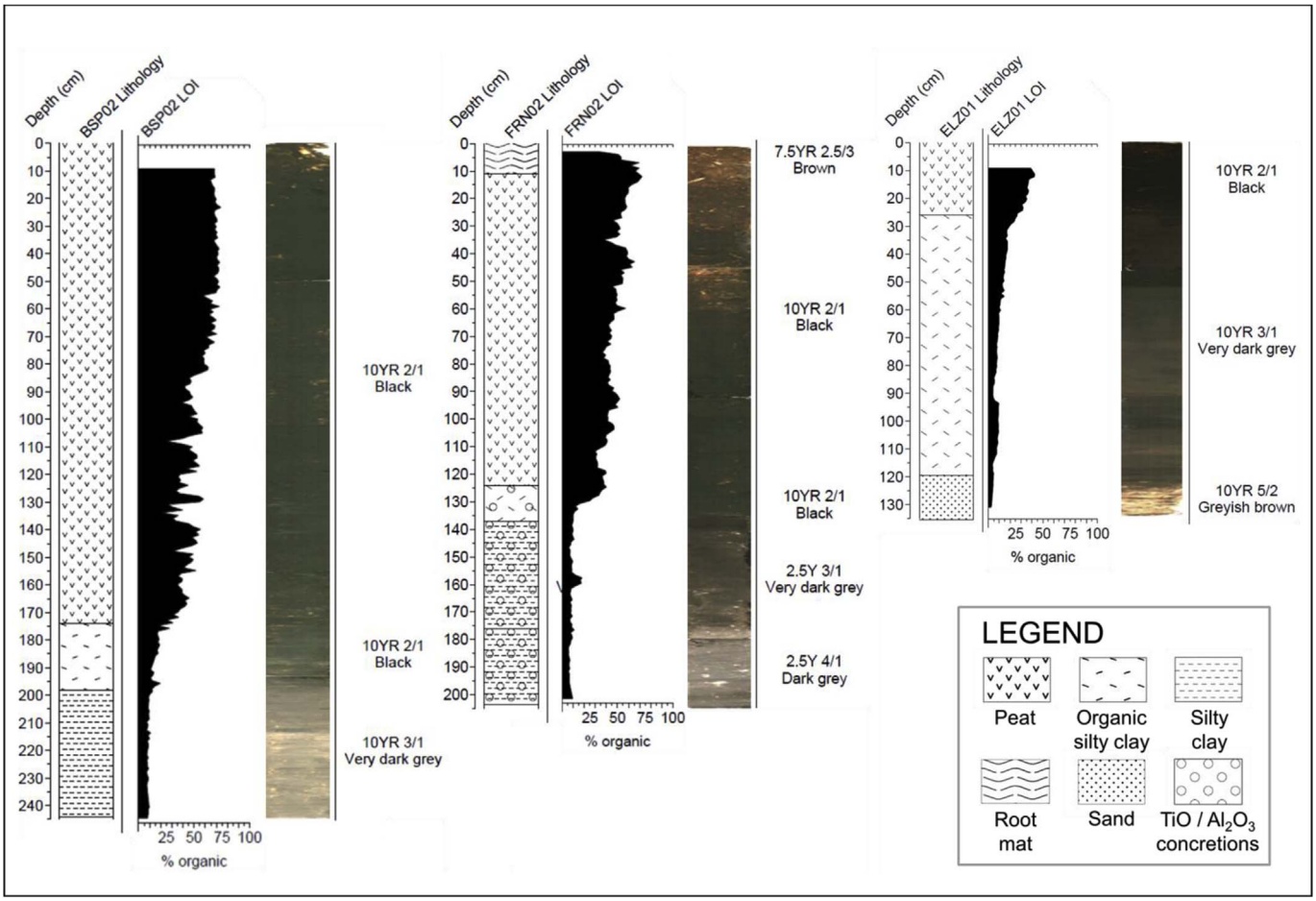

Fig. 6. Generalised stratigraphy, organic content and photographs of cores BSP02, FRN02 and ELZ01.

overlying a sand layer at 120 cm. All three cores have abundant roots throughout.

4.2. Carbon-14 dates

All results from ^{14}C analysis are presented in Table 1 and Fig. 7. Dates are presented in the text as the upper and lower limits of all the possible calibrated age ranges at 2σ (cal. yr BP). Carbon-14 dates of different carbon fractions in the cores at the same or similar depths, in some cases, returned different ages (Fig. 7). Consequently the age structure of each carbon fraction in each core is described in the following sections.

4.2.1. BSP02

Carbon-14 ages for BSP02 range from 1543 to 14,085 cal.yr BP, although age ranges for various carbon fractions differ. All of the fractions where multiple ^{14}C dates were obtained display coherent age–depth relationships, i.e. ages increase with depth (Fig. 7A), with the exception of the root fragments at the base of the core (sample Beta-426,153, 240.5 cm), which are younger than the dates above (younger than all other dates returned below ~100 cm). It should be noted that macro-charcoal dates begin plateauing towards the base of the core. Samples OZT912 and OZT913 record overlapping age ranges (9677–10,189 and 9967–10,250 cal.yr BP, respectively) despite the two ages being 34.5 cm apart.

Dates from identical or similar depths on various carbon fractions returned differing results. For example, macro-charcoal and pollen at 111 cm and 113.5 cm returned ages which differed by > 1000 years (7425–7571 and 6218–6404 cal.yr BP, respectively), dates at 186.5–189 cm gave ages of 8548–8971 (pollen), 9677–10,189 (macro-charcoal) and 9900–10,190 cal.yr BP (SPAC), and at the base of the core (221–241.5 cm) ages ranged from 4437 - 4825 (roots), 9929–10,238 (pollen), 9967–10,250 (macro-charcoal), and 13,755–14,085 cal.yr BP (SPAC) (Fig. 7A, Table 1).

Of the four different carbon fractions there is only one instance where age ranges overlap at similar depths. This occurs at 186.5 cm where macro-charcoal returned an age of 9677–10,189 and at 188.5 cm SPAC returned an age of 9900–10,190 cal.yr BP. Although as noted above pollen from a similar depth recorded a younger age.

4.2.2. BSP00

Ages for the BSP00 core (McGowan et al., 2012; Field et al., 2017) display a very different pattern to those from BSP02 despite both cores being collected from the same spring (Black Springs). Ages in the top 95 cm of BSP00 increase with depth, however these are older than ages for comparative depths in the top ~150 cm of BSP02. For example, in BSP00 sample Wk-29129 at 79.5 cm returns a date of 7659–7833 cal.yr BP, > 4400 years older than sample Wk-44690 extracted from BSP02 at a depth of 75 cm (3040–3227 cal.yr BP).

Below 95 cm (9001–9252 cal.yr BP) ^{14}C dates in BSP00 show no coherency with depth (Fig. 7B). Dates on both pollen and bulk organic material display scattered ages ranging between approximately 6033 and 8341 cal.yr BP.

4.2.3. FRN02

Carbon-14 ages for different carbon fractions in FRN02 displayed high variability, with the occurrence of age reversals in some. Of the three fractions on which multiple ^{14}C dates were obtained (macro-

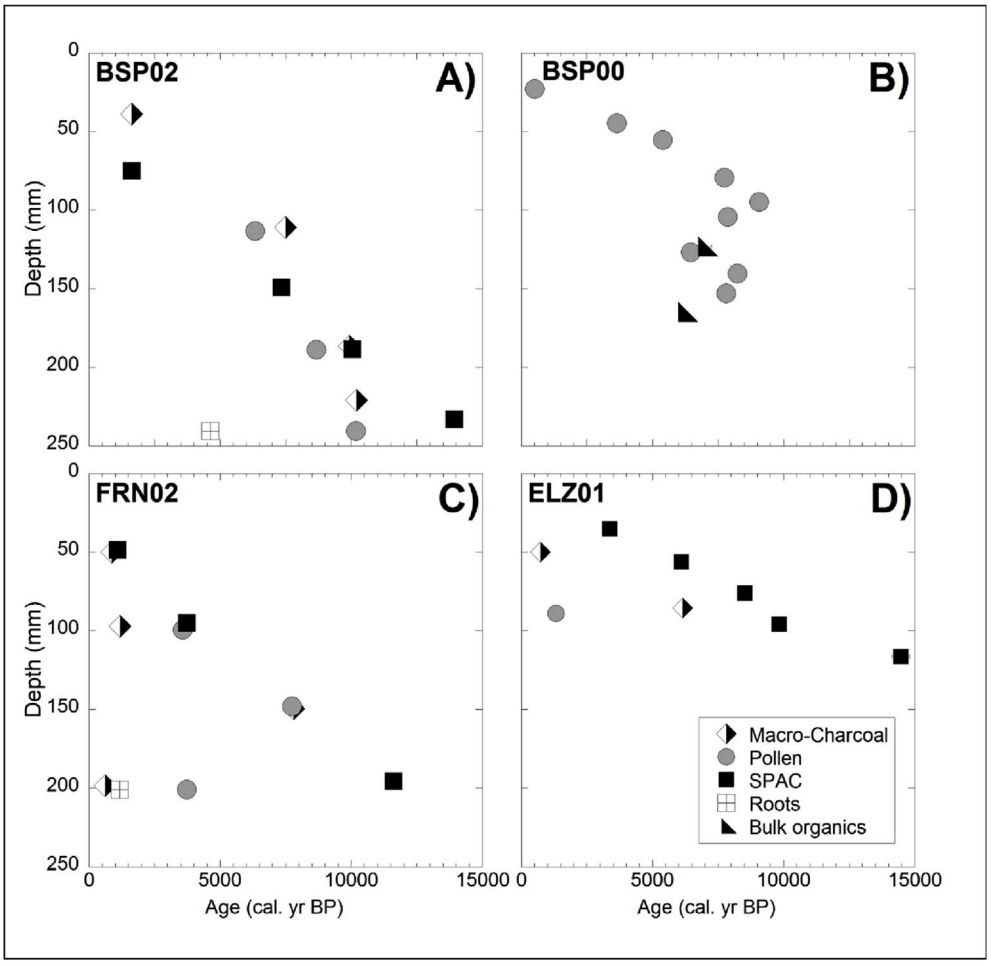

Fig. 7. Calibrated ^{14}C dates for (A) BSP02, (B) BSP00, (C) FRN02 and (D) ELZ01. The 2σ calibrated age ranges are plotted, however in most cases these are not visible at the plotted resolution. These age ranges are provided in Table 1.

charcoal, pollen and SPAC), only SPAC returned sequentially older ages with depth, ranging from 983 to 1177 cal.yr BP at 48.5 cm to 11,357–11,814 cal.yr BP at 195.5 cm and spanning ~10,800 years (Fig. 7C).

By comparison with SPAC, macro-charcoal ages in FRN02 varied by only ~7600 years, and of particular note, the youngest date (sample OZT919) occurred at the greatest depth (553–673 cal.yr BP at 198.25 cm).Pollen dates similarly showed little coherency with depth. While the upper two dates at 99.5 cm and 148 cm broadly displayed the same age–depth relationship as SPAC, the deepest date was anomalously young. The pollen dates also spanned a relatively narrow age range (~4400 years) compared to SPAC.

Of the four different carbon fractions there are three instances where dates are close to or overlap one another. At 48.5 cm SPAC returned an age of 983–1177 and at 50 cm macro-charcoal returned an age of 801–956 cal.yr BP. At 95 cm SPAC returned an age of 3637–3835 cal.yr BP and at 99.5 cm pollen returned an age of 3466–3697 cal.yr BP, although macro-charcoal from a similar depth was younger (1089–1276 cal.yr BP at 97 cm). Finally, at 148 cm pollen returned an age of 7666–7848 cal.yr BP and macro-charcoal returned an age of 7430–8182 cal.yr BP at 149.5 cm.

Overall, and similar to both BSP02 and BSP00, ^{14}C ages in FRN02 were most variable at the base of the core. Dates on roots and macro-charcoal returned ages < 1300 cal.yr BP, pollen 3612–3857 cal.yr BP and SPAC 1068–1271 cal.yr BP.

4.2.4. ELZ01

In core ELZ01 three carbon fractions were dated: macro-charcoal, pollen and SPAC. The five dates returned on SPAC exhibited consistently older ages with depth through the core ranging from 3251 to 3443 cal.yr BP at 35 cm to 14,129–14,811 cal.yr BP at 116 cm (Fig. 7D).

Macro-charcoal dates also returned ages increasing with depth, although diverged from SPAC ages. For example, at 50 cm macro-charcoal was dated at 680–793 cal.yr BP (sample OZT914) compared to SPAC ages of 3251–3443 cal.yr BP and 5946–6265 cal.yr BP above it at 35 cm (sample OZU456) and below it at 56 cm (sample OZU457). Similarly, a macro-charcoal age of 5996–6304 cal.yr BP at 85.5 cm is younger than SPAC ages at 76 and 95.75 cm of 8424–8599 and 9686–10,151 cal.yr BP respectively. A 1297–1365 cal.yr BP age on pollen at 89 cm is younger still.

4.3. Lead-210 profiles and modelled ages

Samples from the top 7 cm of BSP02 and FRN02 and the top 305 mm of ELZ01 were analysed for ^{210}Pb activities for the purposes of building a ^{210}Pb chronology. The results of the ^{210}Pb analysis are presented in Fig. 8. For simplicity, in most instances in the following text errors (2σ) are not described and median depths and activities are used.

In BSP02 supported ^{210}Pb activities are both very high and variable, ranging from 484 to 950 Bq/kg. Due to these high activities and their associated errors, it is difficult to discern unsupported ^{210}Pb activity in the core. Three samples (at 3.75, 4.75 and 6.75 cm) have apparent negative unsupported ^{210}Pb activity. These samples have ^{226}Ra activity in excess of ^{210}Po activity, i.e. there is no measurable unsupported ^{210}Pb in these samples.

The top five samples in BSP02, representing the top 2.75 cm of the core, exhibit a decay profile with depth with unsupported ^{210}Pb activity

Table 1
^{14}C dates and calibrated ages for all samples from cores BSP02, FRN02, ELZ01 and BSP00.

Lab. ID	Fraction dated	Median depth (cm)	Pre-treatment	^{14}C age (BP)[a]	Calibrated age (cal. yr BP)[b,c,d]	Calibrated age range[b,c]
BSP02						
OZT910	Macro-charcoal	39	AAA	1760 ± 30	***1543 - 1709 (100%)***	1543–1709
Wk-44690	SPAC	75	HyPy	3014 ± 20	***3060 - 3227 (99.6%)***	3040–3227
					3040 - 3043 (0.4%)	
OZT911	Macro-charcoal	111	AAA	6630 ± 40	***7425 - 7571 (100%)***	7425–7571
OZT166	Pollen	113.5	AAA	5560 ± 40	***6273 - 6404 (95.1%)***	6218–6404
					6218 - 6236 (4.9%)	
Wk-44691	SPAC	149	HyPy	6430 ± 23	***7258 - 7420 (100%)***	7258–7420
OZT912	Macro-charcoal	186.5	AAA	8890 ± 60	***9677 - 10,189 (100%)***	9677–10,189
Wk-44692	SPAC	188.5	HyPy	8944 ± 29	***9900 - 10,190 (100%)***	9900–10,190
OZT165	Pollen	189	AAA	7910 ± 45	***8548 - 8788 (89.2%)***	8548–8971
					8830 - 8864 (4.6%)	
					8917 - 8971 (5.4%)	
					8886 - 8894 (0.8%)	
OZT913	Macro-charcoal	221	AAA	9065 ± 50	***10,154 - 10,250 (95.8%)***	9967–10,250
					9967 - 9983 (4.2%)	
OZU455	SPAC	233	HyPy	12,100 ± 40	***13,755 - 14,085 (100%)***	13,755–14,085
OZT164	Pollen	240.5	AAA	9030 ± 45	***10,121 - 10,238 (68.3%)***	9929–10,238
					9929 - 9996 (18.1%)	
					10,004 - 10,064 (13.6%)	
Beta-426,153	Roots	240.5	AAA	4140 ± 45	***4437 - 4825 (100%)***	4437–4825
BSP00						
Wk-29127	Pollen	23	AAA	516 ± 35	***493 - 546 (100%)***	493–546
Wk-28374	Pollen	45.5	AAA	3455 ± 30	***3572 - 3726 (92%)***	3572–3821
					3793 - 3821 (6.1%)	
					3750 - 3763 (1.9%)	
Wk-29128	Pollen	55.5	AAA	4671 ± 32	***5343 - 5466 (76.1%)***	5298–5466
					5298 - 5337 (23.9%)	
Wk-29129	Pollen	79.5	AAA	6938 ± 37	***7659 - 7833 (100%)***	7659–7833
Wk-28376	Pollen	95	AAA	8186 ± 35	***9001 - 9145 (84.5%)***	9001–9252
					9166 - 9252 (15.5%)	
Wk-29130	Pollen	104.5	AAA	7081 ± 40	***7786 - 7961 (98.9%)***	7763–7961
					7763 - 7772 (1.1%)	
Wk-41825	Bulk	118.2	AAA	6151 ± 84	***6746 - 7248 (100%)***	6746–7248
Wk-28377	Pollen	127	AAA	5713 ± 30	***6397 - 6537 (98.4%)***	6354–6537
					6354 - 6364 (1.6%)	
Wk-29131	Pollen	140.5	AAA	7439 ± 36	***8161 - 8341 (98.2%)***	8068–8341
					8068 - 8082 (1.8%)	
Wk-28375	Pollen	153	AAA	7033 ± 31	***7707 - 7934 (100%)***	7707–7934
Wk-41826	Bulk	164.8	AAA	5437 ± 22	***6178 - 6284 (91.6%)***	6033–6284
					6120 - 6147 (7.9%)	
					6033 - 6036 (0.5%)	
FRN02						
OZU460	SPAC	48.5	HyPy	1215 ± 25	***1047 - 1119 (49.8%)***	983–1177
					1128 - 1177 (25.2%)	
					983 - 1030 (25%)	
OZT918	Macro-charcoal	50	AAA	1030 ± 30	***801 - 956 (100%)***	801–956
OZU461	SPAC	95	HyPy	3505 ± 25	***3637 - 3835 (100%)***	3637–3835
OZT916	Macro-charcoal	97	AAA	1315 ± 30	***1089 - 1276 (100%)***	1089–1276
OZT163	Pollen	99.5	AAA	3395 ± 40	***3466 - 3697 (100%)***	3466–3697
OZT162	Pollen	148	AAA	6960 ± 40	***7666 - 7848 (100%)***	7666–7848
OZT917	Macro-charcoal	149.5	AAA	6980 ± 210	***7430 - 8182 (100%)***	7430–8182
OZU462	SPAC	195.5	HyPy	10,110 ± 35	***11,392 - 11,814 (99.1%)***	11,357–11,814
					11,357 - 11,373 (0.9%)	
OZT919	Macro-charcoal	198.25	AAA	700 ± 40	***553 - 673 (100%)***	553–673
OZT161	Pollen	201	AAA	3510 ± 40	***3612 - 3857 (100%)***	3612–3857
Beta-426,153	Roots	201	AAA	1290 ± 30	***1068 - 1271 (100%)***	1068–1271
ELZ01						
OZU456	SPAC	35	HyPy	3175 ± 25	***3322 - 3407 (68.9%)***	3251–3443
					3251 - 3305 (26.3%)	
					3426 - 3443 (4.8%)	
OZT914	Macro-charcoal	50	AAA	875 ± 30	***680 - 793 (100%)***	680–793
OZU457	SPAC	56	HyPy	5355 ± 35	***5987 - 6211 (95.9%)***	5946–6265
					5946 - 5969 (2.5%)	
					6247 - 6265 (1.6%)	
OZU458	SPAC	76	HyPy	7790 ± 35	***8424 - 8599 (100%)***	8424–8599
OZT915	Macro-charcoal	85.5	AAA	5440 ± 60	***5996 - 6304 (100%)***	5996–6304
OZT169	Pollen	89	AAA	1475 ± 25	***1297 - 1365 (100%)***	1297–1365
Wk-44693	SPAC	95.75	HyPy	8859 ± 33	***9686 - 9960 (79%)***	9686–10,151
					10,056 - 10,151 (15.5%)	
					9987 - 10,043 (5.5%)	
OZU459	SPAC	116.25	HyPy	12,430 ± 45	***14,129 - 14,811 (100%)***	14,129–14,811

[a] 1σ errors are given for ^{14}C ages (reported at 68% probability).
[b] 2σ errors are given for calibrated ages (reported at 95.4% probability).

[c] Calibrated against SHCal13 (Hogg et al., 2013) with OxCal V.4.2.4 (Bronk Ramsey, 2013).
[d] Since calibration of ^{14}C years to calendar years can result in a number of age ranges, the calibrated age ranges encompassing the largest proportion of total probability (%) are shown in bold and italicised font.

decreasing from 153 to 11 Bq/kg, however uncertainty is high (± 54–89 Bq/kg) (Fig. 8A). Despite this, ages were calculated for these five samples using the CIC and CRS models. The CIC model gives ages ranging from 2011 ± 4–1939 ± 31 CE, indicating that each 5 mm sample slice represents a mean age of 12.7 years, whilst the CRS model gives ages ranging from 2011 ± 2–1989 ± 55 CE, with each sample representing a mean age of 19.5 years (Fig. 9A).

In FRN02 supported ^{210}Pb activities are also very high and variable, ranging from 181 to 487 Bq/kg and giving an apparent negative unsupported ^{210}Pb activity for one sample from 0.25 cm. However, unsupported ^{210}Pb activities increase with depth in the top 7 cm (from −90–441 Bq/kg) (Fig. 8B) making it impossible to construct a ^{210}Pb chronology for this core.

In ELZ01 supported ^{210}Pb activities are high and variable, reaching > 270 Bq/kg in the top 7 cm of the core though it is noteworthy that the supported ^{210}Pb activities are generally lower in ELZ01 than in BSP02 and FRN02. Unsupported ^{210}Pb activities for ELZ01 are much higher than in BSP02 and FRN02, and stabilise at ~400 Bq/kg below 10 cm. In addition, below 10 cm the supported and unsupported ^{210}Pb activities are close (e.g. at 22.75 and 27.75 cm), with counting errors even overlapping for some samples (e.g. at 20.25 cm).

Unsupported ^{210}Pb activities in ELZ01 generally decrease with depth in the top 7.75 cm of the core (from 1620 to 267 Bq/kg) (Fig. 8C). However, there are data points which do not conform to the general relationship. Despite some uncertainty in the decay profile, particularly below 8 cm, ages were calculated for the top 7.75 cm of the core using the CIC and CRS models. The age models indicate that the upper ~7 cm of ELZ01 is < 60 years old, however ages returned from the two models diverge sharply with depth (e.g. the CIC age at 7.75 cm is 1963 ± 5 CE whilst the CRS age at the same depth is 1983 ± 6 CE). The CIC model gives ages ranging from 2013 ± 2–1963 ± 5 CE indicating that each 5 mm sample slice represents a mean age of 3.3 years, whilst the CRS model gives ages ranging from 2014 ± 1–1983 ± 6 CE indicating a mean sample age of 2 years (Fig. 9B). These errors for the ELZ01 ^{210}Pb chronologies are smaller than those for BSP02.

4.4. Plutonium-239 + 240 profiles

Plutonium-239 + 240 activities were analysed in the top 9–12 cm of cores BSP02 and ELZ01 only, since these regions of the core exhibited a general trend of decreasing unsupported ^{210}Pb activity with depth. Results are presented in Fig. 10. For simplicity, in most instances errors are not described in the text and median depths and activities are used.

Activities of $^{230+240}Pu$ were measured in the top 9 cm of the BSP02 core, which based on the CRS modelled ^{210}Pb results should indicate a date between 1950 and 1850 CE, i.e. the lowest sample on which $^{239+240}Pu$ was measured should pre-date atomic testing fallout. Plutonium-239 + 240 activities range from 0.04 to 0.13 (± 0.001–0.003) Bq/kg. Although these activities display a weak trend of increasing with depth, they show no discernible peak. In addition, because activities did not approach zero at 9 cm, no chronostratigraphic markers could be identified.

In the ELZ01 core $^{239+240}Pu$ activities were measured in the top 12 cm, and range from 0.18 to 0.66 (± 0.003–0.011) Bq/kg. They display a generalised bell curve shape characteristic of fallout radionuclide deposition in sediments with a peak in activity at 8.25 cm (0.66 Bq/kg) which could possibly be attributed to the 1963 CE peak in fallout Pu in the Southern Hemisphere (UNSCEAR, 2000). However, due to the structure of the $^{239+240}Pu$ activity through the core and the

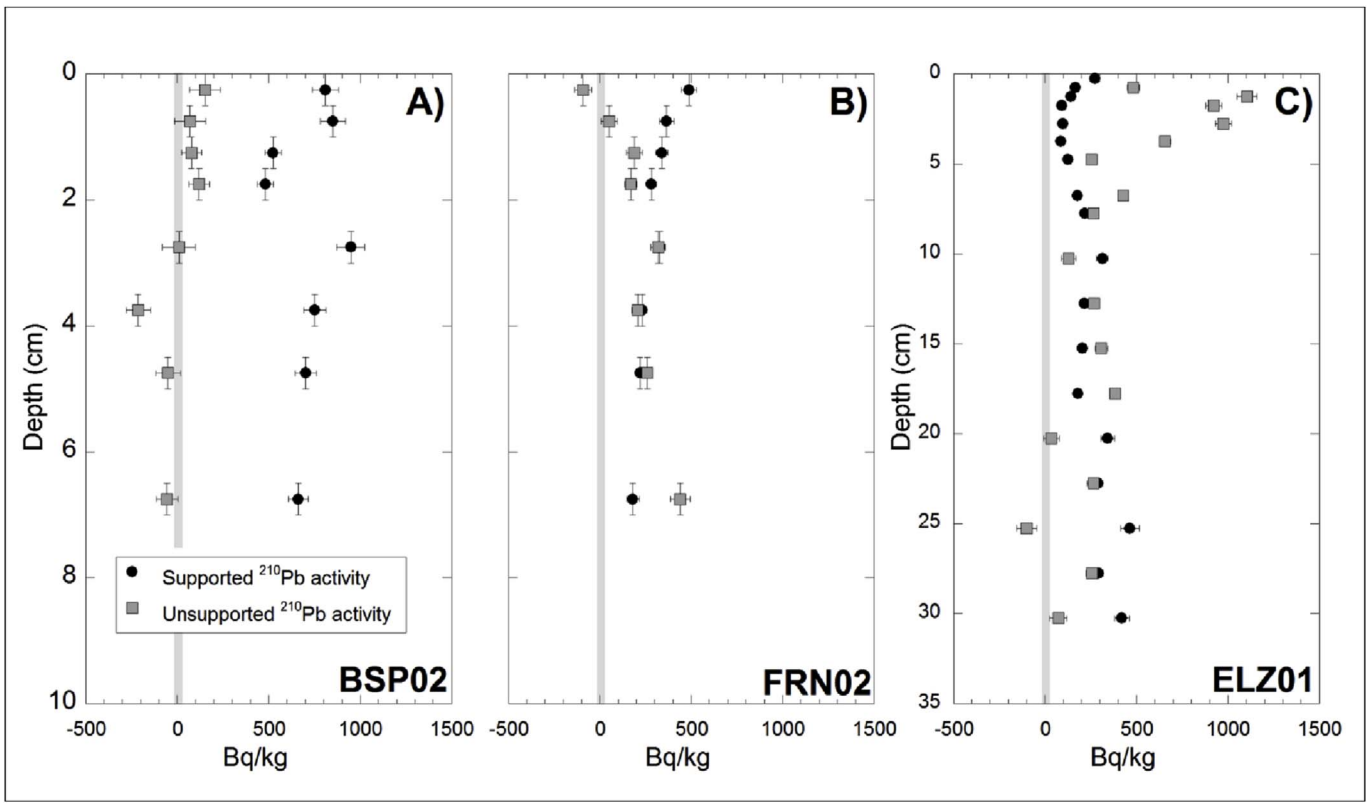

Fig. 8. Supported and unsupported ^{210}Pb activities for (A) BSP02 (B) FRN02 and (C) ELZ01. The grey bar at 0 Bq/kg highlights apparent negative unsupported ^{210}Pb activities. X-axis error bars represent the 2σ error, y-axis error bars represent the sampling depth range.

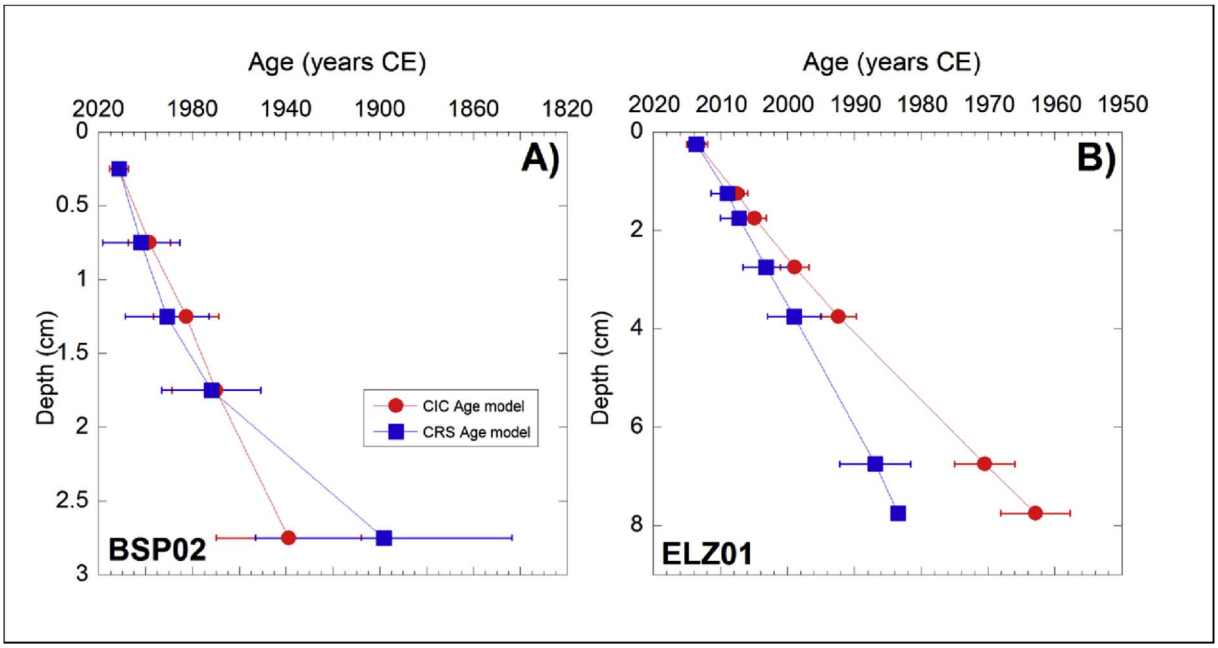

Fig. 9. Lead-210 derived age models for (A) BSP02 and (B) ELZ01.

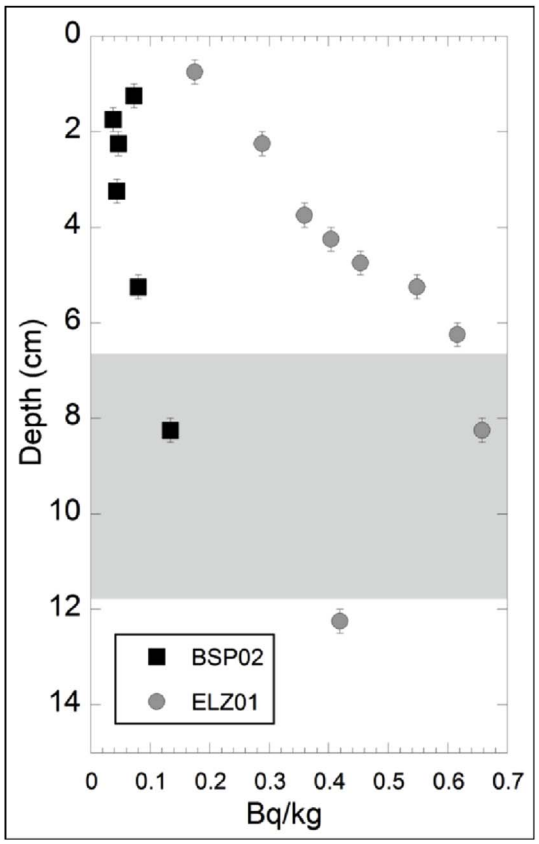

Fig. 10. Plutonium-239 + 240 depth profiles for BSP02 and ELZ01. X-axis errors bars represent the 1σ error, y-axis error bars represent sampling depth range. The grey box indicates the potential range of depths over which peak $^{239+240}$Pu activity may occur in ELZ01 given the sampling resolution and activity profile.

sampling frequency, the peak in the $^{239+240}$Pu may have occurred anywhere between 6.75 and 11.75 cm (Fig. 10). The peak is also relatively broad suggesting that there may have been mixing processes at play, either through chemical migration or through physical sediment mixing from processes such as bioturbation. Despite this, the overall shape of the activity profile remains broadly as would be expected for fallout radionuclides in Australia (Longmore et al., 1983), and the presence and depth of the maximum deposition do not appear to have been affected given the relatively small proportion of the peak that is being redistributed. Because $^{239+240}$Pu activities do not reach background within the sampled range (activity ≤ measurement error) the additional chronometric anchor of the onset of atomic testing fallout in the early 1950s could not be established.

4.5. L_n/T_n profiles for BSP02

The BSP02 L_n/T_n profiles for quartz (BSL) and feldspar (IRSL) are shown in Fig. 11. Values presented in the figure and following text are averaged across the three aliquots.

Both the BSL and IRSL profiles show a general structure of increasing L_n/T_n with depth, however there is a region of increased variability between ~80 and 150 cm. This region of complexity also has higher BSL/IRSL ratios (2–7) compared to the rest of the core where ratios are predominantly ≤2, while it is also marked by relatively high variability in organic content. There is also a sharp increase in L_n/T_n values between 75.5 and 85.5 cm, concurrent with a decrease in organic content (from ~60% to ~42%). Additionally, between ~183.5–215.5 cm there are two L_n/T_n values which are lower than the values surrounding them, i.e. < 5 versus > 5 for the sediment surrounding them.

5. Discussion

5.1. The behaviour of ^{210}Pb and $^{239+240}$Pu in organic spring deposits and their utility for developing chronologies

Used in combination, ^{210}Pb ages and $^{239+240}$Pu activities have the potential to provide detailed chronologies for the past 100 years of spring development. However, in BSP02 use of $^{239+240}$Pu as a chronostratigraphic maker is complex because no clear $^{239+240}$Pu activity peak conforming to peak fallout at 1963 CE could be identified. Furthermore, the onset of atmospheric nuclear weapon testing and the corresponding appearance of a $^{239+240}$Pu signal found in southern hemisphere environmental archives at ~1951 CE (Koide et al., 1979, 1985) could not be established. Activities of $^{239+240}$Pu increase slightly

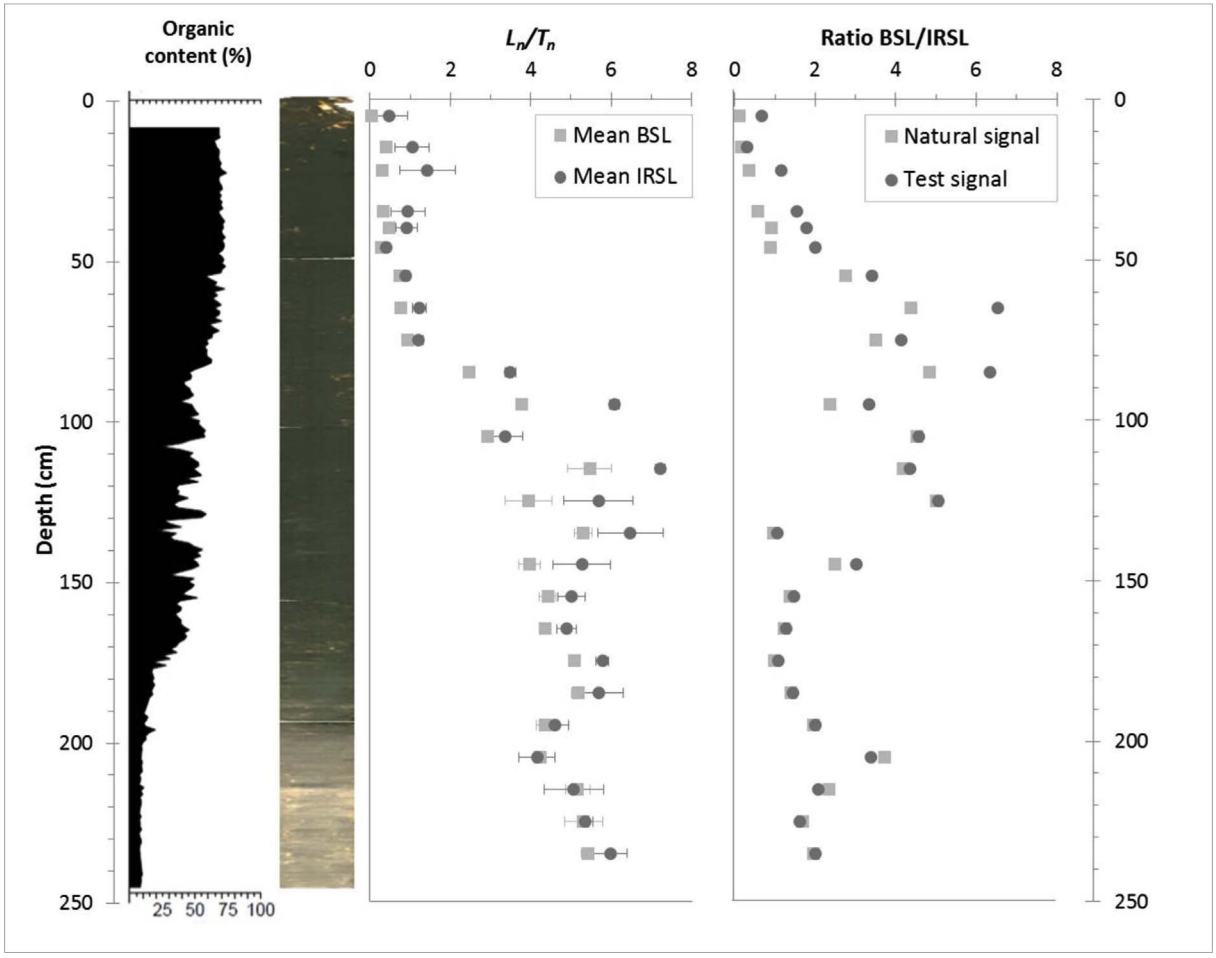

Fig. 11. Quartz (BSL) and feldspar (IRSL) L_n/T_n profiles within BSP02. The organic content and photograph of this core are included for comparison.

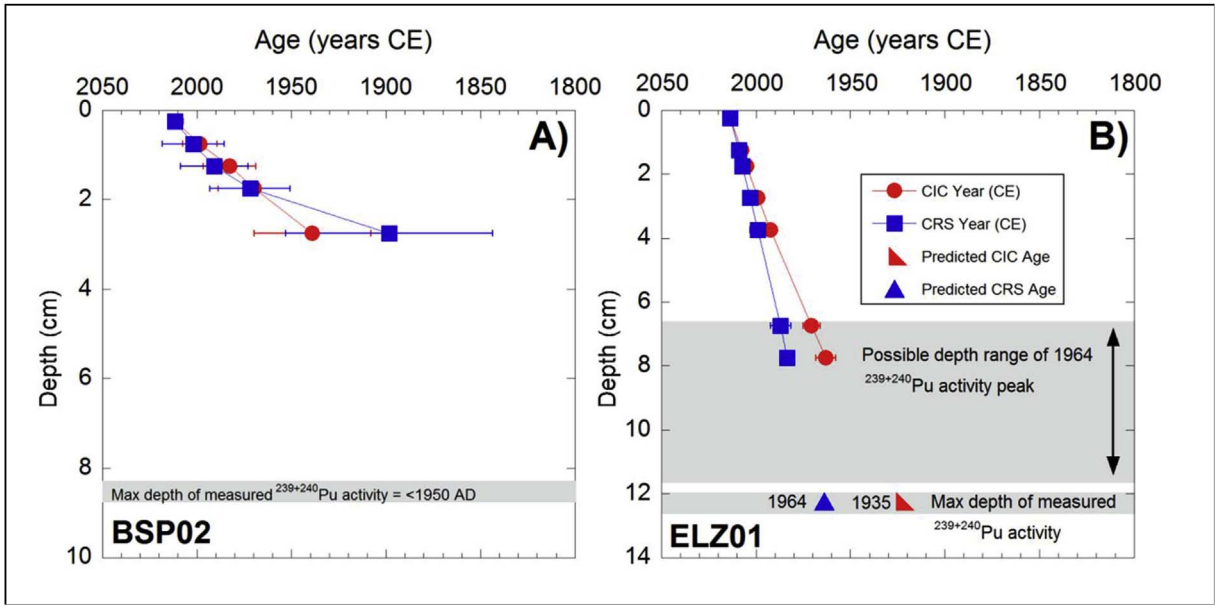

Fig. 12. The comparison of ^{210}Pb chronologies and $^{239+240}$Pu chronostratigraphic information for (A) BSP02 and (B) ELZ01.

down profile, raising the possibility that peak $^{239+240}$Pu activity occurs below 8.25 cm (where the lowermost sample was analysed). Taking $^{239+240}$Pu activity at face value therefore implies that sediment above 8.25 cm should be younger than 1951 CE. By comparison, however, the CIC and CRS ^{210}Pb age models indicate that the fallout period should be constrained within the top 2.75 cm of the core. Therefore there are significant discrepancies between the ^{210}Pb and $^{239+240}$Pu systems. This is illustrated further by extrapolating these models to 8.25 cm (the

maximum depth at which $^{239+240}$Pu activities were analysed) whereby they return dates of 1795 and 1004 CE respectively (Fig. 12). This implies either the ^{210}Pb chronologies are incorrect, which is possible as the high supported ^{210}Pb activities are potentially convoluting the unsupported ^{210}Pb activities, or alternatively that Black Springs may not be recording atmospheric input of Pu, or there may be mixing of Pu between stratigraphic layers.

Plutonium-239 + 240 activities in ELZ01 depict a peak in activity at 8.25 cm which could be attributed to the 1963CE peak in fallout Pu in the Southern Hemisphere (UNSCEAR, 2000). However, the low frequency of sampling between 6.75 and 11.75 cm may mean the precise position of the fallout signal cannot be established (the depth range over which the peak may occur is indicated by the grey box in Fig. 10). Despite this, $^{239+240}$Pu activity in the lowermost analysed sample (at 12.25 cm) implies this depth should equate to a date younger than 1951 CE. Based upon the existing results the CIC ^{210}Pb age model seems to be the best fit for the Pu fallout peak, indicating the 8.25 cm layer to have been deposited in the early 1960s. However, by comparison the CRS model attributes this layer to the 1980s (Fig. 12). Extrapolation of the CIC and CRS modelled ages to lowest depth in which $^{230+240}$Pu activity was measured (12.25 cm) returns dates of 1935 and 1964 CE respectively, however quite clearly the activity at this layer does not suggest a first appearance of fallout, rather a midway point on the rising limb. Therefore the CIC model suggest this depth is too old by comparison to the $^{230+240}$Pu activity record, whereas the CRC model implies the depth is too young. The combination of these factors make it difficult to determine which age model is most accurate based upon the first appearance of fallout Pu.

Lead-210 activity in the spring deposits of ELZ01, FRN02 and BSP02 is very high by comparison to ^{210}Pb fallout rates measured at locations close to the Kimberley. Annual ^{210}Pb fallout measured at Port Headland (~1000 km south of the Kimberley) and Darwin (~650 km northwest of the study sites) (see Turekian et al., 1977) imply that spring ^{210}Pb activity is generally higher than that attributable to atmospheric fallout alone. Lead-210 activities in ELZ01, in particular, are up to three orders of magnitude higher the estimated contribution from atmospheric fallout. Only BSP02 appears to record ^{210}Pb activity which is consistent with (although still higher than) atmospheric fallout rates, i.e., the upper part of the spring records activities of approximately 7500 Bq/m^3/yr, versus the estimated fallout contribution of 800–2200 Bq/m^3/yr. This implies an additional source of ^{210}Pb to the springs.

Overall, despite the reasonable agreement between ^{210}Pb ages and $^{239+240}$Pu markers in ELZ01, the behaviour of both ^{210}Pb and $^{239+240}$Pu is not straightforward, e.g. in BSP02 there are high supported ^{210}Pb activities and considerably lower unsupported ^{210}Pb activities, and no agreement with $^{239+240}$Pu markers, while increasing unsupported ^{210}Pb activities with depth in FRN02 made it impossible to construct a ^{210}Pb chronology for this core. It should also be noted that supported ^{210}Pb values were also relatively high in ELZ01 and in some cases resulted in apparent negative unsupported ^{210}Pb activities.

One possible explanation for the high activities of ^{210}Pb recorded in the spring deposits is that they represent an open system in terms of uranium behaviour. As previously described in Section 1.1, uranium leached from host rocks in solution in groundwater appears to be being absorbed by organic decomposition products (i.e. fulvic and humic acids) which then bind strongly with clay minerals in organic sediments (e.g. Heijnis, 1992; Heijnis and van der Plicht, 1992; Zayre et al., 2006). Consequently, uranium and its daughter products are concentrating in the organic spring deposits. This process does not require high concentrations of U-series elements in groundwater as continual groundwater input will result in progressive enrichment (e.g. Armands, 1967), which appears to be the case here. For example, ^{210}Po and ^{226}Ra activities in spring water filtrate (groundwater) from Black Springs, Fern Pool and Gap Springs had activities of ^{210}Po and ^{226}Ra three orders of magnitude lower than activities in the residues (organic material) (Table 2).

Table 2
Polonium-210 and ^{226}Ra activities of groundwater at Black Springs, Fern Pool and Gap Springs.

Filtrate	^{210}Po (Bq/kg)[a,b]	^{226}Ra (Bq/kg)[a,b]
Black Springs	< 0.02	0.03 ± 0
Fern Pool	< 0.02	< 0.02
Gap Springs	0.03 ± 0.01	< 0.02
Residue	**^{210}Po (Bq/kg)[a,b]**	**^{226}Ra (Bq/kg)[a,b]**
Black Springs	880 ± 35	748 ± 63
Fern Pool	911 ± 38	663 ± 57
Gap Springs	953 ± 42	397 ± 33

[a] 2σ error.
[b] 1 mL is equivalent to 1 g.

The concentration of U-series elements in organic spring deposits is likely to be enhanced by comparison to other mires because of near-constant movement of groundwater through these systems. This explains the enrichment of ^{210}Pb in the springs by comparison to estimated atmospheric fallout. Furthermore the convoluted relationship between supported and unsupported ^{210}Pb activity in the springs, most notably in FRN02, implies the assumption of equilibrium between U-series elements may be violated. That is, different U-series elements may behave differently within the springs, e.g. ^{226}Ra and ^{210}Po from which supported and unsupported ^{210}Pb activities are calculated.

The greater agreement between ^{210}Pb and $^{239+240}$Pu, combined with the more conventional behaviour of ^{210}Pb in ELZ01 by comparison to BSP02 and FRN02, may result in part from the characteristics of sediments between the springs. That is, considerably lower organic contents in ELZ01 in comparison to BSP02 and FRN02 (~35%–40% organic content in the upper sediments of ELZ01 versus ~60%–73% in the upper sediments of BSP02 and FRN02; see Fig. 6) may result in fewer fulvic and humic acids in ELZ01 and therefore lower concentration of uranium. However, it is also noteworthy that the highest ^{210}Pb activity occurred in ELZ01, suggesting caution needs to be used when interpreting these results.

Since upwelling groundwater is a characteristic of all organic spring deposits, it is likely that the problems encountered with ^{210}Pb chronologies in this study will be experienced in similar groundwater influenced systems elsewhere. However, since regions with humid climatic conditions and periods of high rainfall favour enhanced weathering and leaching of uranium (Halbach et al., 1980) the local climate at individual organic springs, alongside local geology, hydrology and organic contents of the spring sediments themselves will influence the concentration and behaviour of U-series elements. It is therefore essential to consider these factors before attempting to build ^{210}Pb chronologies in organic spring deposits.

5.2. The behaviour of different carbon fractions in organic springs

The reliability of the pollen concentrate, macro-charcoal, bulk organic and SPAC fractions for ^{14}C dating are discussed below using down-profile characteristics of each fraction and comparisons between them (i.e. the likelihood that each ^{14}C date accurately represents the age of sediment accumulation). Additionally, the "visual" best fit between the ^{14}C and L_n/T_n datasets for BSP02 is depicted in Fig. 13. This is used to compare ^{14}C age–depth relationships to the L_n/T_n profile which can be assumed to reflect relative patterns in the geochronological history of sediment accumulation in the core.

Across the three dated spring systems pollen concentrate dates behave inconsistently. In FRN02 there are two cases where pollen concentrates return age ranges close to, or overlapping with other carbon fractions, suggesting that those particular dates may be reliable, although FRN02 pollen returns reversals in age below 148 cm. Aside from the two dates in FRN02, pollen concentrate dates from the cores

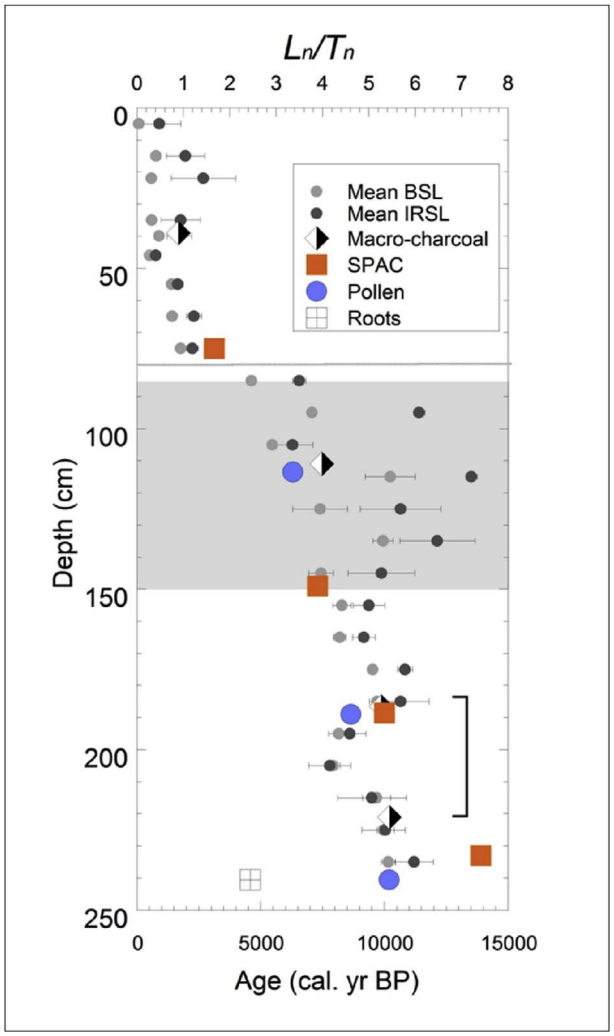

Fig. 13. Quartz (BSL) and feldspar (IRSL) L_n/T_n profiles for BSP02 alongside ^{14}C dates from all carbon fractions (macro-charcoal, SPAC, pollen and roots). A possible growth hiatus region is depicted by the grey line, the region of increased variability in the L_n/T_n data is indicated by shading, and the shift to lower L_n/T_n towards the base of the core is defined by brackets.

collected in 2015 are younger than comparable dates from other carbon fractions (with the exception of the basal root samples), although pollen dates from BSP02 do show a coherent age–depth relationship (Fig. 13). Additionally, despite cores BSP00 and BSP02 being collected from the same spring (Black Springs), pollen ages from the two cores display different patterns. That is, in BSP00 pollen ages (and bulk organics) below 95 cm display an erratic age–depth relationship. Consequently, ^{14}C dates from pollen concentrate show a complex pattern in the studied springs and are assumed, in most instances, not to be reflecting their chronostratigraphic development.

Like pollen, macro-charcoal dates behave differently across the three springs. In BSP02 the age-depth profile of macro-charcoal closely follows L_n/T_n (Fig. 13), and across the cores collected in 2015 there are three instances where macro-charcoal age ranges are close to or overlap those from other carbon fractions, suggesting these particular ages are reliable. However, in FRN02 ages on macro-charcoal are extremely convoluted with a large reversal in age returned below 149.5 cm. In BSP02 and ELZ01 macro-charcoal predominantly displays older ages with depth, indicating that dates may generally be reflecting the chronostratigraphic development of the springs. Despite this, in most instances the macro-charcoal ages are significantly different from other carbon fractions. This indicates that the macro-charcoal dates should be treated with caution.

All ages returned from SPAC following HyPy pre-treatment are older than comparable dates from other carbon fractions. There are three cases where SPAC age ranges are close to or overlap those of other carbon fractions, and in addition, SPAC is the only carbon fraction which displays consistently older ages with depth across all of the spring systems studies. Since SPAC represents the carbon fixed by pyrolysis at the time of the burning event (Ascough et al., 2009) it is an "indigenous" component of the original charcoal and is therefore likely to produce a reliable ^{14}C date (Bird et al., 2014). Whilst there is evidence, in some cases, that SPAC can be subject to alteration and degradation (e.g. Ascough et al., 2010; Bird et al., 2002), the HyPy pre-treatment has been demonstrated to be effective in removing contaminants; e.g. it has been shown to remove > 92% contamination in charcoal created at temperatures ≥400 °C (Bird et al., 2014). Although a small fraction of pyrolised labile carbon may be lost during HyPy pre-treatment (Wurster et al., 2012) SPAC is therefore less likely to be subject to contamination which may affect other carbon fractions and the "original" age is likely to be better preserved. Given the consistency of SPAC ages within each core and between each spring, this fraction appears to be more reliable in describing chronostratigraphic development of the springs. The only inconsistency in the SPAC ages occurs in the bottom of BSP02 where the oldest SPAC date diverges from the general L_n/T_n profile below 183.5 cm (Fig. 13). The reasons for this discrepancy are discussed in the following sections.

5.3. Sources of ^{14}C anomalies

As discussed in Section 1.1, there are a number of potential processes that could be affecting ^{14}C ages in the studied springs. One possibility is that the chronostratigraphic integrity of the springs is compromised by mixing and overturning. An alternative is that various carbon fractions are contaminated within the springs due to translocation of fractions within the spring profiles, biological activity within the spring sediments, or incorporation of young or old carbon.

5.3.1. The influence of mixing, overturning and erosion on spring chronologies

Processes such as mixing, overturning or erosion could affect the chronostratigraphic integrity of the springs. In the case of highly organic springs, these processes are not often apparent in the sedimentology of the deposit. For this reason the luminescence properties of core BSP02 were analysed by measuring the L_n/T_n signal through that core (Fig. 11). Although not providing ages, the L_n/T_n profile provides an indication of the stratigraphy and age structure of the core. Consequently, overturning or hiatuses in the growth of the spring would be recorded in reversals or step changes in the L_n/T_n ratio. In BSP02 the L_n/T_n profiles exhibit a generalised trend of increasing ratios with depth. This implies that the core has predominantly maintained its chronostratigraphic integrity with no large scale internal mixing of the deposit.

However, the L_n/T_n indicates there are some potential disturbances. The sharp increase in L_n/T_n values between 75.5 and 85.5 cm is indicative of either an unconformity, or a change in mound growth. This change is otherwise undetected in other parameters (e.g. colour and texture). An unconformity could result from removal of material e.g. deflation during periods of increased aridity and sediment desiccation, or scouring during periods of increased precipitation. Alternatively, this may represent a hiatus in spring growth or a decrease in spring productivity, however the latter scenario is at odds with an increase in core organic content above 80 cm (Fig. 11).

Another region of potential spring disturbance can be recognised by high variability in the L_n/T_n ratios between ~80 and 150 cm. In that section of the core the L_n/T_n ratios do not consistently increase with depth, while in addition the BSL and IRSL signals diverge from one another (grey box in Fig. 13). This could represent a partially mixed

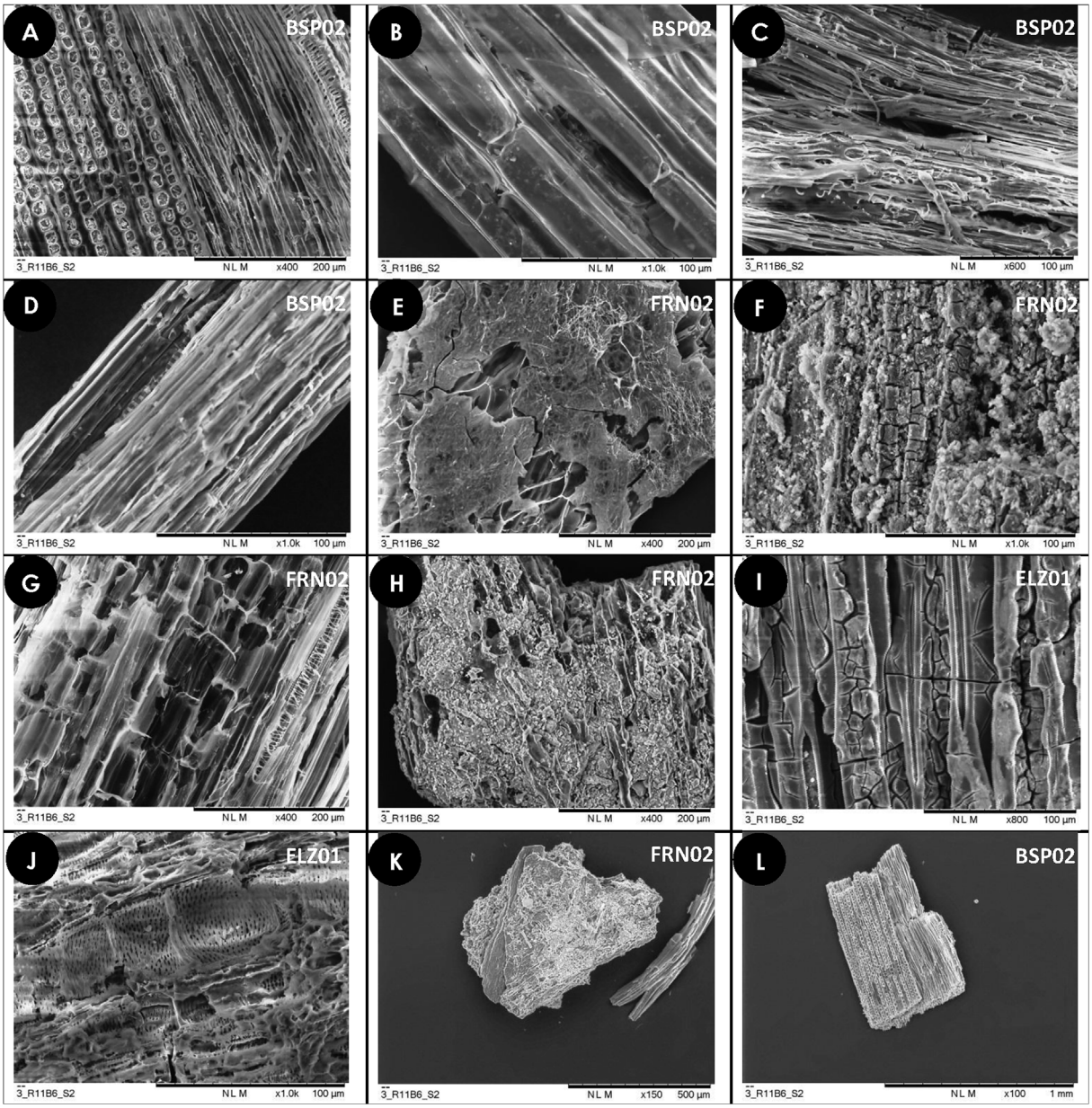

Fig. 14. SEM micrographs of charcoal structure from macro-charcoal ^{14}C samples from BSP02 core: (A) OZT910, (B) OZT911, (C) OZT912, (D) OZT913; FRN02 core: (E) OZT916, (F) OZT917, (G) OZT918, (H) OZT919; ELZ core: (I) OZT914, (J) OZT915; and entire fragments from (K) OZT919 and (L) OZT910.

region of the core by processes such as cracking, self-mulching, bioturbation, slumping or changes in vent position. Divergence in the BSL and IRSL signals may also imply material of a different origin of quartz (BSL) versus feldspars (IRSL) and/or a different depositional history given the greater sensitivity of quartz to bleaching, e.g. more local sediment rather than long-range dust input (e.g. McGowan et al., 2012). Alternatively, these differences could reflect dose rate variations, e.g. corresponding with variable U load associated with integration of groundwater and fluctuating organic content (Fig. 11). Variable dose rates are more likely to have influenced the region between 190 and 220 cm (as indicated on Fig. 13) as this region represents the transition between the more organic section of the core and the silty clay (Fig. 6) in which dose rate fluctuations are most likely due to hydrologic variability.

Despite some minor potential complexity in the chronostratigraphy as indicated by the L_n/T_n data, the overall impression is that the chronostratigraphy is largely intact and is therefore unlikely that severe complications of spring stratigraphy are responsible for the erratic ^{14}C age–depth relationships frequently observed. However, the divergence in ages between different carbon fractions may, in some cases, be attributed to this minor complexity. This is discussed in more detail in the sections that follow.

5.3.2. *The effect of roots on ^{14}C ages*

As described above in Section 3.1 cores BSP02, FRN02 and ELZ01 contained abundant root fragments throughout. The prevalence of roots throughout organic spring deposits is unsurprising since these environments support enhanced plant growth, often with deep rooted vegetation by comparison to the surrounding landscape (Scott and Vogel, 1983). For instance, *Phragmites* is often found growing across organic springs and can have root and rhizome penetration > 1.8 m (Granholm and Chester, 1994). Although both sieving and heavy liquid separation were used to remove these, root fragments were still observed under light microscopy in the < 150 μm size pollen fraction retained for dating.

The presence of roots affecting ^{14}C ages has been noted in numerous

studies. As previously mentioned, initial ^{14}C ages at Florisbad Spring, South Africa were assumed to be influenced by root contamination (Kuman and Clarke, 1986). Efforts to remove root fragments (by hand) from bulk organic ^{14}C samples resulted in different ages and, importantly, a consistent stratigraphic chronology at this site (Scott and Nyakale, 2002) implying that roots were a source of contamination. Similarly, a microscopic search of spring sediments from Rietvlei in South Africa revealed that abundant minute rootlets were at depths concurrent with anomalous ^{14}C dates (Scott and Vogel, 1983). Roots have therefore been frequently credited with contaminating ^{14}C dates from organic spring deposits in a variety of global locations (e.g. Butzer, 1984a,b; Kuman and Clarke, 1986; Van de Geer, 1986; Boyd, 1990b; Scott et al., 2003; Field et al., 2017).

The ages returned by the roots in BSP02 and FRN02 were considerably younger than corresponding dates from other carbon fractions (with the exception of macro-charcoal in FRN02 which is younger than the roots for reasons discussed in Section 5.3.3). Ages on roots at the base of BSP02 also diverged from the L_n/T_n profile (Fig. 13) suggesting that they do not reflect the true age of sediment accumulation.

As described in Section 1.1 roots can facilitate the transport of young carbon into older stratigraphic units via a number of processes. Consequently the pollen concentrate ages, which were consistently younger than other carbon fractions, are considered likely to be contaminated by the introduction of young carbon from root fragments retained within the pollen fraction. The ages on bulk organics may be similarly affected. Furthermore, roots are able to penetrate large charcoal fragments (Harkness et al., 1994) so it is possible that minute fragments also affected the macro-charcoal ages.

In the studied springs, root contamination is likely to be most severe in the deepest stratigraphic units of organic spring deposits since those roots have been present for longer periods of time and may be decomposed, making them particularly difficult to differentiate from the surrounding organic sediment (Scott et al., 2003). In BSP02, BSP00 and FRN02 the most variable dates are in the lower stratigraphic units suggesting that this is the case.

5.3.3. Groundwater effects on ^{14}C ages

Inspection of charcoal fragments from the studied springs by optical microscopy revealed that they were sometimes soft and coated with a light-coloured waxy residue, i.e. they lacked the vitreous lustre typical of charcoal. This was particularly the case for FRN02. Subsequent examination by an SEM equipped with EDXA further revealed charcoal fragments in FRN02 generally had a degraded structure by comparison to those in cores BSP02 and ELZ01 (Fig. 14), although this was not ubiquitous in all charcoal fragments recovered from FRN02 (see Fig. 14G). EDXA showed that the altered charcoal fragments from FRN02 contain a more complex chemical structure, most notably with large concentrations of aluminium, phosphorus, silicon and sodium (Fig. 15). This was most apparent in two dated samples from FRN02 (OZT917 and OZT919 - Fig. 14F and H respectively, and Fig. 15). In these samples C comprised < 30% of OZT917 and < 40% of OZT919, while the fragments contained inclusions of Al (> 7%), Si (4–8%) and P (1–5%). By contrast, charcoal from BSP02 appeared relatively unaltered and contained higher concentrations of C (57–67%), with only minor concentrations of Si and S present (< 2%). Other charcoal samples from ELZ01 (OZT914 and OZT915) and FRN02 (OZT918) showed no obvious visual alteration (Fig. 14I and G respectively), but still contained relatively high concentrations of Na (3% in OZT914), Si (2% in OZT918), P (~1% in all), and Al (4% in OZT915) (Fig. 15) implying some possible minor alteration.

Consistent with the presence of more altered charcoal, ^{14}C ages on macro-charcoal from FRN02 returned similar ages from different depths which were much younger than ages returned on other carbon fractions. In particular, sample OZT919 was visually degraded and contained high concentrations of other elements. It returned a pronounced reversal in age (Fig. 15) in comparison to all other ^{14}C ages from the core. The less altered charcoal in sample OZT918 returned an age close to that of SPAC (sample OZU460). Alteration of charcoal has previously been reported at Nauwaliabila I in the Northern Territory (Bird et al., 2002). Optical microscopy, SEM and EDXA investigation in that case also revealed that charcoal fragments were soft, heavily coated by iron oxides and clays and had severely degraded internal structures and high abundances of elements other than carbon (e.g. iron, aluminium and oxygen) (Bird et al., 2002). This was concluded to result from ongoing replacement of the original charcoal by iron and aluminium oxides and oxihydroxides. Subsequent macro-charcoal ^{14}C dates from Nauwaliabila I were considered to be inconsistent with the likely chronostratigraphy (Bird et al., 2002).

As described in Section 1.1, alteration of charcoal in high weathering environments, such as northern Australia, is facilitated by the large surface area and porous nature of charcoal. This enables the *in-situ* contamination by young carbon through the adsorption of organic or inorganic compounds which can move in solution through the sediment (Bird, 2007), or through oxidative processes (Cohen-Ofri et al., 2006) mediated by microbial activity and photo-oxidation (particularly in coarser sediment matrixes) (Bird et al., 1999). Since water tables in springs typically fluctuate in response to climatic variability (Scott, 2016) charcoal may be altered by these processes in organic spring deposits. It is therefore likely that the charcoal alteration observed in the Kimberley springs has affected the ^{14}C ages, as evidenced by younger macro-charcoal ages in comparison to SPAC ages in FRN02 and ELZ01. Because charcoal will also comprise a portion of any bulk organic samples and can be broken down into finer fractions (Walker, 2005; Bird, 2007) it is likely that it is also present in pollen concentrate (e.g. Mensing and Southon, 1999).

At the Nauwaliabila I site in the Northern Territory altered charcoal occurred alongside authigenic pisolites and altered quartzite fragments. This implied that charcoal alteration resulted from water table fluctuations (Bird et al., 2002). It is likely that the same mechanism was responsible for the charcoal alteration observed in FRN02 and ELZ01. The TiO/Al_2O_3 concretions in FRN02 are indicative of water table variations, with similar concretions observed in dehydrating conditions (Sherman, 1952). That these are only present in FRN02 indicates that groundwater fluctuations have been most pronounced at this site, again consistent with the greatest degree of charcoal alteration.

5.3.4. Allochthonous transport of old charcoal

As previously discussed, ^{14}C dates on pollen concentrate, bulk organics and even macro-charcoal are likely to have been compromised by additions of young carbon. It is also possible that old carbon may be reintroduced by, for example, aeolian and alluvial deposition. This potentially affects the lowest SPAC ^{14}C date in BSP02, where this age is distinct from the L_n/T_n profile (Fig. 13). As previously discussed in Section 3.1, the lower units of BSP02 consist of less organic material. These sediments were deposited early in the development of the spring, predominantly by alluvial (and to a lesser extent, aeolian) deposition (e.g. Field et al., 2017). The difference between this SPAC age (sample OZU455) and the L_n/T_n ratios in the lower stratigraphic unit may therefore reflect the incorporation of “old” charcoal remobilised from the surrounding landscape and transported into the spring largely by alluvial processes. There is also a risk that finer “old” charcoal may be incorporated via aeolian processes at any stage of spring growth. Since the SPAC was extracted by HyPy from bulk sediment samples there was no way to differentiate whether it is derived from macroscopic or microscopic charcoal (the latter reflecting the fine fraction). However, there are two results where SPAC ^{14}C age ranges are close to or overlap macro-charcoal ^{14}C dates, suggesting that the SPAC in all but the deepest stratigraphic units (e.g. BSP02) is relatively uncompromised by “old” fine fractions.

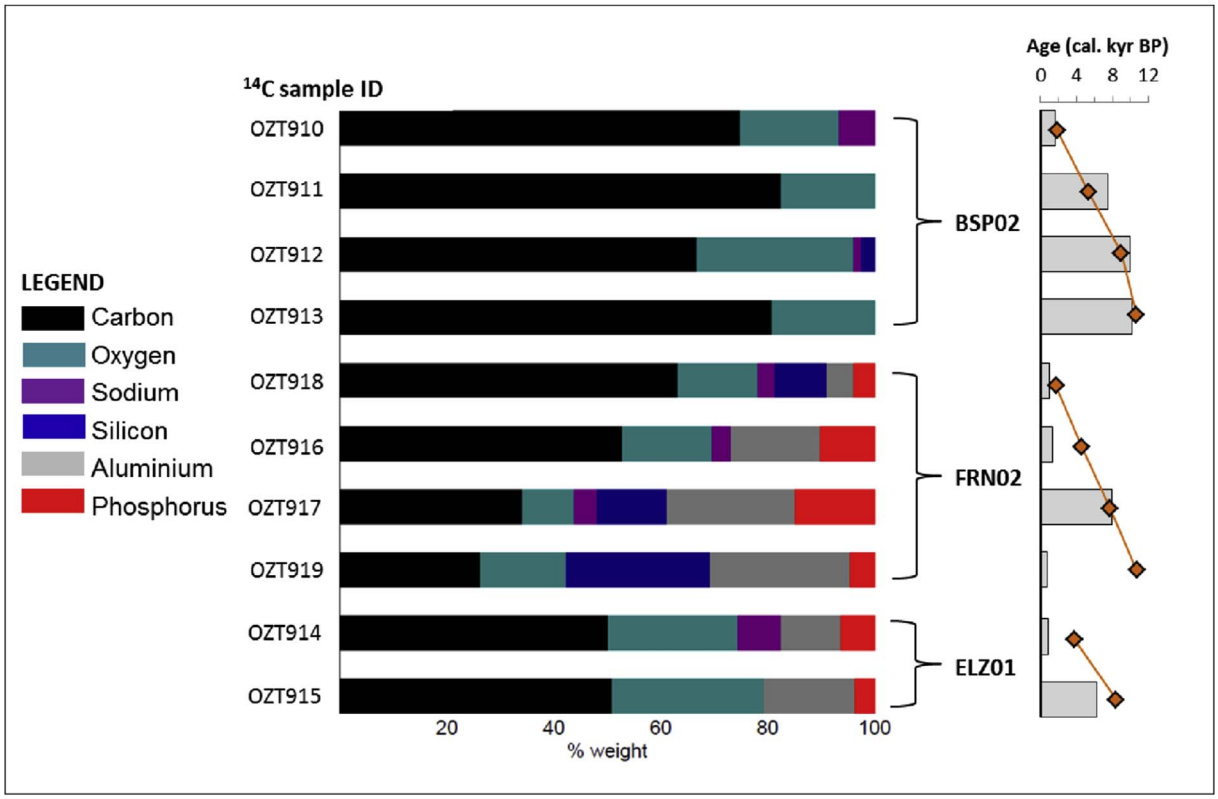

Fig. 15. Elemental composition (% by weight) of charcoal fragments from macro-charcoal ^{14}C samples in Kimberley springs. Samples are plotted alongside their calibrated ages (shown as grey bars) and depth-sequences (shown as orange lines) for comparison. (For interpretation of the references to colour in this figure legend, the reader is referred to the web version of this article.)

5.4. The feasibility of different carbon fractions for building reliable ^{14}C chronologies in organic spring deposits

Results presented here show that in organic spring deposits there are a number of processes which can affect different carbon fractions. There is therefore value in dating multiple fractions to both refine the chronology of these archives and to understand how processes within spring environments can affect ^{14}C results.

In these settings root fragments are likely to comprise part of any bulk sediment or pollen concentrate (and potentially even macro-charcoal) sample submitted for ^{14}C dating. Very fine rootlets cannot be easily separated from these carbon fractions via chemical or physical pre-treatment (e.g. density separation or acid digestion) without also removing the target material for dating. Whilst it appears that roots can be removed from organic spring deposits by hand with successful results (e.g. Scott and Nyakale, 2002), removing root fragments in this way is not always possible since the extremely time consuming nature of this task would make it impractical for most studies. It is also likely that very small or light coloured fragments may be missed, particularly in deeper stratigraphic units where roots may be indistinguishable from the surrounding matrix (Scott et al., 2003).

In organic spring deposits macro-charcoal can be contaminated by organic/inorganic compounds and oxidation via fluctuations in groundwater, a process inherent in spring systems (Scott, 2016), however these contaminants often appear impossible to remove by AAA pre-treatments (e.g. Gillespie et al., 1992; Harkness et al., 1994; Higham et al., 2009a,b), or potentially even more aggressive oxidation stepped combustion techniques such as ABOX-SC (e.g. Bird et al., 2002). It is therefore essential to assess the suitability of charcoal prior to ^{14}C analysis since ages will be unreliable where there is post-depositional alteration. It is important to note that this alteration is not always visually apparent and that SEM micrographs alone are insufficient to discern it. Therefore EDXA or similar should also be used to assess the suitability of the charcoal fraction prior to use, however we note such investigation may prove too time consuming for most studies. Given the abundance of roots throughout organic spring deposits, even when there is no evidence of alteration, charcoal ages should be interpreted with caution as it is possible that roots may have penetrated charcoal fragments targeted for dating (Harkness et al., 1994). As charcoal is likely to comprise part of bulk organic and pollen concentrate samples, where alteration exists this will contribute to inaccuracies in ^{14}C dates from these fractions.

Overall, SPAC isolated by the HyPy pre-treatment is the most successful means to remove contamination introduced by roots, groundwater fluctuations and associated weathering that would otherwise result in erroneous ages. These results presented from Black Springs and Fern Pool, along with those from other spring studies, suggest that the effects of carbon contamination in springs becomes more pronounced with time, that is dates from the bottom lower sections of springs on different carbon fractions show the greatest degree of variability (Figs. 2, 3 and 7). The implication of this has been that while, in some cases, it has been possible to extract some palaeoenvironmental information from proxy data sets within springs, developing reliable chronologies for the lower sections of springs has been problematic (e.g. Butzer, 1984a,b; Van de Geer et al., 1986; Scott, 1987; Macphail et al., 1999; Scott et al., 2003; Dobrowolski et al., 2012; Fluin et al., 2013; Mazurek et al., 2014; Field et al., 2017). Consequently, in some studies palaeoenvironmental reconstructions have only been produced for the top section of springs (e.g. McGowan et al., 2012), while in other studies (e.g. Field et al., 2017) age models, based on reliable ages from the top sections of springs, have been extrapolated to older sections. These approaches have obvious limitations in terms of record length and reliability. The results presented here suggest HyPy provides a means of reliably building chronologies within complex spring environments, thereby placing environmental and climatic changes on more secure timescales throughout the entire spring sedimentary

record. HyPy as a technique is also advantageous as it is rapid and efficient, requiring no prior or additional pre-treatments (physical or chemical) prior to dating, that is, following HyPy the sample can be converted directly to CO_2 (Ascough et al., 2010). Furthermore, HyPy has a high degree of measurement precision (Ascough et al., 2009; Meredith et al., 2012). However, in juvenile springs SPAC may be contaminated by "old" allochthonous charcoal.

6. Conclusions

This study demonstrates that in complex hydro-geological settings such as springs, there is a need to understand how different dating components are behaving. It also shows value in utilising multiple radionuclides for understanding spring behaviour and developing accurate chronologies for their sediments. This is important since, despite the complexity of organic spring deposits as highlighted by this study, they are critical palaeoenvironmental archives in many settings. Therefore, developing accurate geochronology is crucial for understanding past environments.

This study reveals that in organic spring deposits there are multiple sources of contamination which can convolute ^{14}C chronologies, and highlights that not one single carbon fraction appears to be universally reliable. Pollen concentrate, bulk organic and macro-charcoal fractions are unsuitable for obtaining accurate ^{14}C dates in these settings due to contamination introduced by roots and groundwater fluctuations. In some cases, macro-charcoal pre-treated with the AAA technique may be appropriate where it has not undergone post-depositional alteration, although it is essential that charcoal fragments are examined for contamination. However, groundwater fluctuations inherent in spring environments limit the use of this approach, and the investigation of macro-charcoal is likely to be too time consuming to be practical in most cases. Alternatively, the HyPy pre-treatment methodology is a rapid, effective method for the removal of several primary sources of geochronological complexity, and can isolate unaltered SPAC from charcoal likely giving reliable ^{14}C dates in deposits of well-developed organic springs. There is a risk, however that "old" carbon may be incorporated in juvenile spring sediments, and that a small fraction of the labile carbon component may also be pyrolysed during HyPy treatment. The former is not an issue specific to the HyPy pre-treatment methodology but rather, to the spring environment and will affect all age determinations using ^{14}C.

Providing age control for recent spring sediments via ^{210}Pb methodologies may prove more difficult due to post-burial enrichment by uranium which is common to organic sediments in open systems such as springs. The degree of enrichment is likely to vary between individual springs based on organic content of the sediments, local hydrological and climatic conditions, and geology. These parameters should be taken into account when considering the use of ^{210}Pb analysis for age determination.

We therefore recommend using a combination of methods to build chronologies for organic spring deposits including HyPy to isolate SPAC for ^{14}C analysis, circumstantial evidence, and auxiliary datasets such as ^{210}Pb, $^{239+240}Pu$ and L_n/T_n. The ability to construct reliable chronologies in these settings will facilitate the correct interpretation of palaeoenvironmental, palaeoclimatic, archaeological and palaeontological records. This is of particular importance in arid and semi-arid environments which contain few sites other than organic springs suitable for building continuous records of environmental and climatic change. Although our study pertains to springs, the contamination pathways described here are not exclusive to these systems and our results are likely widely applicable to other settings,.e.g. swamps or marshes experiencing significant seasonal changes in hydrology and deep root growth. Accordingly, this also highlights that caution should be exercised in the interpretation of age models from similar sites and environmental settings where pollen, charcoal and bulk organic samples have been used for ^{14}C dating.

Acknowledgements

This research was supported by the Kimberley Foundation Australia with 2015 fieldwork and the majority of the laboratory research completed whilst the first author was the recipient of an Australian Postgraduate Award, an ANSTO Postgraduate Research Award (ANSTO PGRA No. 2158493), and a Kimberley Foundation Top-Up Scholarship. We acknowledge the financial support from the Australian Government for the Centre for Accelerator Science at ANSTO through the National Collaborative Research Infrastructure Strategy (NCRIS) and would like to extend thanks to laboratory staff at ANSTO, in particular to Fiona Bertuch, Daniela Fierro, Brodie Cutmore and Jack Goralewski for assistance with sample preparation and measurement. We would also like to express our gratitude to Patricia Gadd at ANSTO for the procurement of core imagery using the ITRAX core scanner. We would also like to thank Alan Hogg and Fiona Petchey at Waikato Radiocarbon Dating Laboratory for their advice regarding their pre-treatment methodologies. We are indebted to Michael Bird at James Cook University for his guidance concerning charcoal contamination and the HyPy pre-treatment methodology, and to Sandra Rodrigues and Laura Phillips at The University of Queensland for assistance with the identification of the concretions of titanium and aluminium oxide in FRN02. We would also like to recognise Linda Nothdurft at The University of Queensland for her assistance with the SEM and EDXA. We also thank Thomas Higham and an anonymous reviewer for their comments which improved this manuscript. Finally, we would like to extend a special thank you to the Koeyers family of Drysdale River Station and the Lacey family of Mt Elizabeth Station for providing excellent local knowledge and hospitality during the 2015 field campaign, and to Andy Hammond and the late Grahame Walsh for collecting the BSP00 core.

References

Appleby, P.G., Oldfield, F., 1978. The calculation of 210Pb dates assuming a constant rate of supply of unsupported 210Pb to the sediment. Catena 5 (1), 1–8.
Armands, G., 1967. Geochemical prospecting of a uraniferous bog deposit at Masugnsbyn, northern Sweden. In: Kvalheim, A. (Ed.), Geochemical Prospecting in Fennoscandia. Interscience, New York, pp. 127–154.
Ascough, P.L., Bird, M.I., Brock, F., Higham, T.F.G., Meredith, W., Snape, C.E., Vane, C.H., 2009. Hydropyrolysis as a new tool for radiocarbon pre-treatment and the quantification of black carbon. Quat. Geochronol. 4, 140–147.
Ascough, P.L., Bird, M.I., Meredith, W., Wood, R.E., Snape, C.E., Brock, F., Higham, T.F.G., Large, D., Apperley, D., 2010. Hydropyrolysis: implications for radiocarbon pre-treatment and characterization of black carbon. Radiocarbon 52, 1336–1350.
Backwell, L.R., McCarthy, T.S., Wadley, L., Henderson, Z., Steininger, C.M., deKlerk, B., Barré, M., Lamothe, M., Chase, B.M., Woodborne, S., Susino, G.J., Bamford, M.K., Sievers, C., Brink, J.S., Rossouw, L., Pollarolo, L., Trower, G., Scott, L., d'Errico, F., 2014. Multiproxy record of late Quaternary climate change and Middle Stone Age human occupation at Wonderkrater, South Africa. Quat. Sci. Rev. 99, 42–59.
Bird, M.I., 2007. Charcoal. In: Elias, S.A., Mock, C.J. (Eds.), Encyclopedia of Quaternary Science, second ed. Elsevier, pp. 2950–2958.
Bird, M.I., Moyo, E., Veenendaal, E., Lloyd, J.J., Frost, P., 1999. Stability of elemental carbon in a savanna soil. Glob. Biogeochem. Cycles 13, 923–932.
Bird, M.I., Turney, C.S.M., Fifield, L.K., Jones, R., Ayliffe, L.K., Palmer, A., Cresswell, R., Robertson, S., 2002. Radiocarbon analysis of the early archaeological site of Nauwalabila I, Arnhem Land, Australia: implications for sample suitability and stratigraphic integrity. Quat. Sci. Rev. 21, 1061–1075.
Bird, M.I., Levchenko, V., Ascough, P.L., Meredith, W., Wurster, C.M., Williams, A., Tilston, E.L., Snape, C.E., Apperley, D.C., 2014. The efficiency of charcoal decontamination for radiocarbon dating by three pre-treatments – ABOX, ABA and HyPy. Quat. Geochronol. 22, 25–32.
Boyd, W.E., 1990a. Mound springs. In: Tyler, M.J., Twidale, C.R., Davies, M., Wells, C.B. (Eds.), Natural History of the North East Deserts. Royal Society of South Australia Inc, pp. 107–118 no. 6.
Boyd, W.E., 1990b. Quaternary pollen analysis in the arid zone of Australia: Dalhousie Springs, Central Australia. Rev. Palaeobot. Palynology 64, 331–341.
Boyd, B., Luly, J., 2005. Inland mound springs. In: Whinam, J., Hope, G. (Eds.), The Peatlands of the Australasian Region. (Mires - from Siberia to Tierra del Fuego), pp. 397–434 Biologiezentrum der Oberoesterreichischen Landesmussen.
Bronk Ramsey, C., 2013. OxCal Program, V.4.2.2. Radiocarbon Accelerator Unit. University of Oxford Available at: http://c14.arch.ox.ac.uk/oxcalhelp/hlp_contents.html.
Browne, E., Tuli, J.K., 2006. Nuclear data Sheets for A = 236. Nucl. Data Sheets 107, 2649–2714.
Browne, E., Tuli, J.K., 2007. Nuclear data Sheets for A = 137. Nucl. Data Sheets 108,

2713 2318.
Browne, E., Tuli, J.K., 2014. Nuclear data Sheets for A = 239. Nucl. Data Sheets 122, 293–376.
Bureau of Meteorology, 2016. Climate Data Online. Available at: http://www.bom.gov.au/climate/data/.
Butzer, K.W., 1984a. Archaeogeology and Quaternary environment in the interior of southern Africa. In: Klein, R.G. (Ed.), South African Prehistory and Palaeoenvironments. Balkema, Rotterdam, pp. 64.
Butzer, K.W., 1984b. Late quaternary environments in South Africa. In: Vogel, J.C. (Ed.), Late Cainozoic Palaeoclimates of the Southern Hemisphere. Balkema, Rotterdam, pp. 29.
Child, D.P., Hotchkis, M.A.C., Williams, M.L., 2008. High sensitivity analysis of Plutonium isotopes in environmental samples using Accelerator Mass Spectrometry (AMS). J. Anal. Atomic Spectrom. 23, 765–768.
Cohen-Ofri, I., Weiner, L., Boaretto, E., Mintz, G., Weiner, S., 2006. Modern and fossil charcoal: aspects of structure and diagenesis. J. Archaeol. Sci. 33 (3), 428–439.
Department of Environment and Conservation, 2012. Understanding wetlands. A guide to managing and restoring wetlands in Western Australia – Wetland vegetation and flora, part 2: Kimberley. .
Dobrowolski, R., Hajdas, I., Melke, J., Alexandrowicz, W.P., 2005. Chronostratigraphy of calcareous mire sediments at Zawadówka (eastern Poland) and their use in paleogeographical reconstruction. Geochronometria 24, 69–79.
Dobrowolski, R., Pidek, I.A., Alexandrowicz, W.P., Halas, S., Pazdur, A., Piotrowska, N., Buczek, A., Urban, D., Melke, J., 2012. Interdisciplinary studies of spring mire deposits from Radzików (south Podlasie Lowland, east Poland) and their significance for palaeoenvironmental reconstructions. Geochronometria 39 (1), 10–29.
Dobrowolski, R., Bałaga, K., Buczek, A., Alexandrowicz, W.P., Mazurek, M., Hałas, S., Piotrowska, N., 2016. Multi-proxy evidence of Holocene climate variability in Volhynia Upland (SE Poland) recorded in spring-fed fen deposits from the Komarów site. Holocene 26 (9), 1406–1425.
Dodson, J.R., Wright, R.V.S., 1989. Humid to arid to subhumid vegetation shift on Pilliga Sandstone, Ulungra springs, New south Wales. Quat. Res. 32, 182–192.
Field, E., McGowan, H., Moss, P., Marx, S., 2017. A late Quaternary record of monsoon variability in the northwest Kimberley, Australia. Quat. Int. 449, 119–135.
Fink, D., Hotchkis, M., Hua, Q., Jacobsen, G., Smith, A.M., Zoppi, U., Child, D., Mifsud, C., van der Gaast, H., Williams, A., Williams, M., 2004. The ANTARES AMS facility at ANSTO. Nucl. Instrum. Methods Phys. Res. Sect. B 224, 109–115.
Fluin, J., De Rozario, N., Tibby, J., Gotch, T., Love, A.J., 2013. Palaeo-ecological analysis of artesian springs in the GAB of South Australia. In: In: Gotch, T.B. (Ed.), Allocating Water and Maintaining Springs in the Great Artesian Basin, Volume V: Groundwater-dependent Ecosystems of the Western Great Artesian Basin National Water Commission, Canberra, pp. 1–58.
Gillespie, R., Hammond, A.P., Goh, K.M., Tonkin, P.J., Lowe, D.C., Sparks, R.J., Wallace, G., 1992. AMS radiocarbon dating of a late Quaternary tephra site at Graham's Terrace, New Zealand. Radiocarbon 34, 21–28.
Granholm, J.M., Chester, S.E., 1994. A landowner's Guide to Phragmites Control. The Office of the Great Lakes, Michigan Department of Environmental Quality.
Halbach, P., Von Borstel, D., Gundermann, K.-H., 1980. The uptake of uranium by organic substances in a peat bog environment on a granite bedrock. Chem. Geol. 29, 117–138.
Harkness, D.D., Roobol, M.J., Smith, A.L., Stipp, J.J., Baker, P.E., 1994. Radiocarbon redating of contaminated samples from a tropical volcano: the mansion "Series" of St. Kitts, West Indies. Bull. Volcanol. 56, 326–334.
Harris, C.R., 1981. Oases in the desert: the mound springs of northern South Australia. Proc. R. Geogr. Soc. Aust. South. Aust. Branch 81, 26–39.
Harris, C., 2002. Culture and geography: south Australia's mound springs as trade and communication routes. Hist. Environ. 16 (2), 8–11.
Hatté, C., Morvan, J., Noury, C., Paterne, M., 2001. Is classical acid-alkali-acid treatment responsible for contamination/an alternative proposition. Radiocarbon 43, 177–182.
Head, L., Fullager, R., 1992. Palaeoecology and archaeology in the East Kimberley. Quat. Australasia 10 (1), 27–31.
Heijnis, H., 1992. Uranium/thorium Dating of Late Pleistocene Peat Deposits in NW Europe. Published PhD thesis. University of Groningen, The Netherlands, pp. 149.
Heijnis, H., van der Plicht, J., 1992. Uranium/thorium dating of Late Pleistocene peat deposits in NW Europe, uranium/thorium isotope systematics and open-system behaviour of peat layers. Chem. Geol. 94, 161–171.
Heiri, P., Lotter, A.F., Lemcke, G., 2001. Loss on ignition as a method for estimating organic and carbonate content in sediments: reproducibility and comparability of results. J. Palaeolimnology 25 (1), 101–110.
Higham, T., Brock, F., Peresani, M., Broglio, A., Wood, R., Douka, K., 2009a. Problems with radiocarbon dating the middle to upper palaeolithic transition in Italy. Quat. Sci. Rev. 28 (13–14), 1257–1267.
Higham, T.F.G., Barton, H., Turney, C.S.M., Barker, G., Bronk Ramsey, C., Brock, F., 2009b. Radiocarbon dating of charcoal from tropical sequences: results from the Niah Great Cave, Sarawak, and their broader implications. J. Quat. Sci. 24 (2), 189–197.
Hogg, A.G., Hua, Q., Blackwell, P.G., Niu, M., Buck, C.E., Guilderson, T.P., Heaton, T.J., Palmer, J.G., Reimer, P.J., Reimer, R.W., Turney, C.S.M., Zimmerman, S.R.H., 2013. SHCAL13 southern hemisphere calibration, 0-50,000 years cal BP. Radiocarbon 55 (4), 1889–1903.
Hua, Q., Jacobsen, G.E., Zoppi, U., Lawson, E.M., Williams, A.A., Smith, A.M., McGann, M.J., 2001. Progress in radiocarbon target preparation at the ANTARES AMS centre. Radiocarbon 43 (2A), 275–282.
Hughes, P.J., Lambert, R.J., 1985. The Assessment of Aboriginal Archaeological Significance of Mound Springs in South Australia. Kinhill Stearns for SA Department of Planning and Environment, Adelaide.
Koide, M., Michel, R., Goldberg, E.D., Herron, M.M., Langway, C.C., 1979. Depositional history of artificial radionuclides in the Ross Ice Shelf, Antarctica. Earth Planet. Sci. Lett. 44, 205–223.
Koide, M., Bertine, K.K., Chow, T.J., Goldberg, F.D., 1985. The $^{240}Pu/^{239}Pu$ ratio, a potential geochronometer. Earth Planet. Sci. Lett. 72, 1–8.
Kuman, K., Clarke, R.J., 1986. Florisbad - new investigations at a Middle Stone Age hominid site in South Africa. Geoarchaeology 1, 103–125.
Longmore, M., O'Leary, B., Rose, C., Chandica, A., 1983. Mapping soil erosion and accumulation with the fallout isotope caesium-137. Soil Res. 21, 373–385.
Macphail, M.K., Pemberton, M., Jacobson, G., 1999. Peat mounds of southwest Tasmania: possible origins. Aust. J. Earth Sci. 46, 667–677.
Magee, J.W., Miller, G.H., Spooner, N.A., Questiaux, D., 2004. Continuous 150 k.y. monsoon record from Lake Eyre, Australia: Insolation-forcing implications and unexpected Holocene failure. Geology 32 (10), 885–888.
Mazurek, M., Dobrowolski, R., Osadowski, Z., 2014. Geochemistry of deposits from spring-fed fens in West Pomerania (Poland) and its significance for palaeoenvironmental reconstruction. Geomorphol. relief, Process. Environ. 4, 323–342.
McCarthy, T.S., Ellery, W.N., Backwell, L., Marren, P., de Klerk, B., Tooth, S., Brandt, D., Woodborne, S., 2010. The character, origin and palaeoenvironmental significance of the Wonderkrater spring mound, South Africa. J. Afr. Earth Sci. 58, 115–126.
McGowan, H., Marx, S., Moss, P., Hammond, A., 2012. Evidence of ENSO megadrought triggered collapse of prehistory Aboriginal society in northwest Australia. Geophys. Res. Lett. 39 (22), L22702.
Mensing, S.A., Southon, J.R., 1999. A simple method to separate pollen for AMS radiocarbon dating and its application to lacustrine and marine sediments. Radiocarbon 41 (1), 1–8.
Meredith, W., Ascough, P.L.A., Bird, M.I., Large, D.J., Snape, C.E., Yongge Sun, Y., Tilston, E.L., 2012. Assessment of hydropyrolysis as a method for the quantification of black carbon using standard reference materials. Geochimica Cosmochimica Acta 97, 131–147.
Moss, P.T., 2013. Palynology and its application to geomorphology. In: Shroder, J.F., Switzer, A.D., Kennedy, D.M. (Eds.), Treatise on Geomorphology. Academic Press, San Diego, CA, United States, pp. 315–325.
Munyikwa, K., Brown, S., 2014. Rapid equivalent dose estimation for aeolian dune sands using a portable OSL reader and polymineralic standardised luminescence growth curves: expedited sample screening for OSL dating. Quat. Geochronol. 22, 116–125.
Murray, A.S., Wintle, A.G., 2000. Luminescence dating of quartz using an improved single-aliquot regenerative-dose protocol. Radiat. Meas. 33, 57–73.
Owen, R.B., Renaut, R.W., Hover, V.C., Ashley, G.M., Muasya, A.M., 2004. Swamps, springs and diatoms: wetlands of the semi-arid Bogoria-Baringo Rift, Kenya. Hydrobiologia 518, 59–78.
Ponder, W.F., 1986. Mound springs of the Great Artesian Basin. In: De Deckker, P., Williams, W.D. (Eds.), Limnology in Australia. CSIRO, Dordrecht, pp. 403–420.
Potezny, V., 1978. Survey of Mound Springs between Marree and William Creek. Notes Compiled for the Senior Environmental Officer (Projects). Department for the Environment, Adelaide.
Rambeau, C.M., 2010. Palaeoenvironmental reconstruction in the Southern Levant: synthesis, challenges, recent developments and perspectives. Philosophical Trans. R. Soc. 368, 5225–5524.
Reeves, J.M., Bostock, H.C., Ayliffe, L.K., Barrows, T.T., De Deckker, P., Devriendt, L.S., Dunbar, G.B., Drysdale, R.N., Fitzsimmons, K.E., Gagan, M.K., Griffiths, M.L., Haberle, S.G., Jansen, J.D., Krause, C., Lewis, S., McGregor, H.V., Mooney, S.D., Moss, P., Nanson, G.C., Purcell, A., van der Kaars, S., 2013. Palaeoenvironmental change in tropical Australasia over the last 30,000 years - a synthesis by the OZ-INTIMATE group. Quat. Sci. Rev. 74, 97–114.
Richter, D., Richter, A., Dornich, K., 2013. Lexsyg—a new system for luminescence research. Geochronometria 40, 220–228.
Robbins, J.A., Edgington, D.N., 1975. Determination of recent sedimentation rates in Lake Michigan using Pb-210 and Cs-137. Geochimica Cosmochimica Acta 39, 285–304.
Sanderson, D.C., Murphy, S., 2010. Using simple portable OSL measurements and laboratory characterisation to help understand complex and heterogeneous sediment sequences for luminescence dating. Quat. Geochronol. 5, 299–305.
Scott, L., 1982a. A late quaternary pollen record from the Transvaal Bushveld, South Africa. Quat. Res. 17, 339–370.
Scott, L., 1982b. A 5000-year old pollen record from spring deposits in the bushveld at the north of the Soutpansberg, South Africa. Palaeoecol. Afr. 14, 45–55.
Scott, L., 1987. Late quaternary forest history in Venda, southern Africa. Rev. Palaeobot. Palynology 53, 1–10.
Scott, L., 1988. Holocene environmental change at western Orange Free State pans, South Africa, inferred from pollen analysis. Palaeoecol. Afr. 19, 109–118.
Scott, L., 2016. Fluctuations of vegetation and climate over the last 75000 years in the Savanna Biome, South Africa: Tswaing Crater and Wonderkrater pollen sequences reviewed. Quat. Sci. Rev. 145, 117–133.
Scott, L., Vogel, J.C., 1983. Late quaternary pollen profile from the Transvaal Highveld, South Africa. South Afr. J. Sci. 79, 266–272.
Scott, L., Cooremans, B., 1990. Late Quaternary pollen from a hot spring in the upper Orange River basin, South Africa. South Afr. J. Sci. 86, 154–156.
Scott, L., Nyakale, M., 2002. Pollen indications of Holocene palaeoenvironments at Florisbad spring in the central free state, South Africa. Holocene 12 (4), 497–503.
Scott, L., Holmgren, K., Talma, A.S., Woodborne, S., Vogel, J.C., 2003. Age interpretation of the Wonderkrater spring sediments and vegetation change in the Savanna Biome, Limpopo province, South Africa. South Afr. J. Sci. 99, 484–488.
Sherman, G.D., 1952. The titanium content of Hawaiian soils and its significance. Soil Sci. Soc. Proc. 16 (1), 15–18.
Shotyk, W., 1988. Review of the inorganic geochemistry of peats and peatland waters. Earth Sci. Rev. 25, 95–176.
Sirocko, F., Claussen, M., Litt, T., Sanchez-Goni, M.F., 2007. The Climate of Past

Interglacials. Elsevier, Amsterdam, pp. 1–622.
Stevenson, J., Haberle, S.G., 2005. Macro charcoal analysis: a modified technique used by the Department of archaeology and Natural history. PalaeoWorks Tech. Rep. 5, 8–14.
Szalay, A., 1969. Accumulation of uranium and other micrometals in coal and organic shales and the role of humic acids in these geochemical enrichments. Arkiv Mineralogi Och Geol. 5, 23–35.
Truc, L., Chevalier, M., Favier, C., Cheddadi, R., Meadows, M.E., Scott, L., Carr, A.S., Smith, G.F., Chase, B.M., 2013. Quantification of climate change for the last 20,000 years from Wonderkrater, South Africa: implications for the long-term dynamics of the Intertropical Convergence Zone. Palaeogeogr. Palaeoclimatol. Palaeoecol. 386, 575–587.
Turekian, K.K., Nozaki, Y., Benninger, L.K., 1977. Geochemistry of atmospheric radon and radon products. Annu. Rev. Earth Planet. Sci. 5, 227–255.
UNSCEAR, 2000. Sources and Effects of Ionizing Radiation. United Nations, Vienna, Austria, pp. 649 vol. I.
Van de Geer, G., Colhoun, E.A., Mook, W.G., 1986. Stratigraphy, pollen analysis and paleoclimatic interpretation of Mowbray and Broadmeadows Swamps, north western Tasmania. Aust. Geogr. 17, 121–133.
Van der Wijk, A., El-Daoushy, F., Arends, A.R., Mook, W.G., 1986. Dating peat with U/Th disequilibrium: some geochemical considerations. Chem. Geol. 59, 283–292.
Van Zinderen Bakker, E.M., 1989. Middle stone age palaeoenvironments at Florisbad (South Africa). Palaeoecol. Afr. 20, 133–154.
Veth, P., 1989. Islands in the interior - a model for the colonization of Australia's Arid Zone. Archaeol. Ocean. 24 (3), 81–92.
Walker, M., 2005. Radiometric dating 1:radiocarbon dating. In: Walker, M. (Ed.), Quaternary Dating Methods. John Wiley & Sons, Chichester, pp. 17–55.
Wilcken, K.M., Hotchkis, M., Levchenko, V., Fink, D., Hauser, T., Kitchen, R., 2015. From carbon to actinides: a new universal 1MV accelerator mass spectrometer at ANSTO. Nucl. Instrum. Methods Phys. Res. B 361, 133–138.
Wintle, A., Murray, A., 2006. A review of quartz optically stimulated luminescence characteristics and their relevance in single-aliquot regeneration dating protocols. Radiat. Meas. 41, 369–391.
Wurster, C.M., Lloyd, J., Goodrick, I., Saiz, G., Bird, M.I., 2012. Quantifying the abundance and stable isotope composition of pyrogenic carbon using hydrogen pyrolysis. Rapid Commun. Mass Spectrom. 26, 2690–2696.
Zackrisson, O., Nilsson, M.-C., Wardle, D.A., 1996. Key ecological function of charcoal from wildfire in the Boreal forest. Oikos 77, 10–19.
Zayre, I., Gonzalez, A., Krachler, M., Cheburkin, A.Y., Shotyk, W., 2006. Spatial distribution of natural enrichments of aresenic, selenium, and uranium in a minerotrophic peatland, Gola di Lago, Canton Tichino, Switzerland. Environ. Sci. Technol. 40, 6568–6574.